The Diagramatical Solution of the Two-Impurity Kondo Problem

by

Chen Zhou

Dissertation submitted to the Faculty of the

Virginia Polytechnic Institute and State University

in partial fulfillment of the requirements for the degree of

Doctor of Philosophy

in

Physics

APPROVED:

Ting-Kuo Lee, Co-chairperson	Samuel P. Bowen, Co-chairperson
Clayton D. Williams	Richard H. Zallen
Tom E. Gilmer, Jr.	Royce Zia

August 24, 1988

Blacksburg, Virginia

The Diagramatical Solution of the Two-Impurity Kondo Problem

by

Chen Zhou

Ting-Kuo Lee, Co-chairperson

Samuel P. Bowen, Co-chairperson

Physics

(ABSTRACT)

The problem of the two-impurity Kondo problem is studied via the perturbative diagrammatical method. The high temperature magnetic susceptibility is calculated to fourth order in the coupling constant J for different regimes. The integral equations for the ground state energy are established and solved numerically. The two-stage Kondo effect and corresponding energy scales are found which agree with the scaling results.

Acknowledgements

This dissertation has profited greatly from the members of my committee : Ting-Guo Lee, Samuel Bowen, Laynam Chang, Clayton Williams, Richard Zallan, Royce Zia, and Tom Gilmore jr.. I would like to thank them all for the support and encouragement.

I am grateful especially to T. K. Lee, my advisor, for his guidance, support and patience during the whole course of the dissertation; To Sam Bowen for his support and great deal of time he spent on me and my dissertation; to Laynam Chang for his help and encouragement in many aspects; and to Clayton Williams, for his careful reading and correcting the dissertation.

Most of all, I would like to thank , my dear wife, for her encouragement and understanding over the years and I am indebted to her for her help and support both directly and indirectly for this work.

Table of Contents

List of Illustrations

a). The unoccupied state in which both impurity states are empty. The characteristic energy of the state (fermi energy) is set to be zero.

b). Singly occupied impurity states with one hole in the fermi sea. σ denotes the spin of the impurity. The total degeneracy is four because the occupied impurity can be at either site 1 or site 2 with spin up or spin down. The energy of the states is ε_f (a negative value).

c). The doubly occupied impurity states with two holes in the fermi sea. The energy of the states is $2\varepsilon_f$ and the total degeneracy is also four.

Fig 3. Leading order non-crossing self-energy diagrams for all nine states. The shadowed blocks represent the self-energies of the corresponding states which sandwich the block. The expressions for these self-energies are given in eqs. (4.1).

Fig. 4 Examples of crossed diagrams for the doubly occupied states. Intermediate states are not specified. Fig. 4.(a) is of the order V^6 and Fig. 4.(b) of the order V^8. Each diagram represents a group of diagrams with different intermediate states. All of them should be included in the perturbative calculation.

Fig. 5 An example of a vertex function in terms of integral equations. The shadowed areas represent the vertices. Once again the intermediate states are not specified.

Fig. 6 A family of crossed diagrams for the unoccupied state. These diagrams are of leading order in 1/N because there are no restrictions on the summation for

the intermediate states. They represent dominant terms in the ground state energy.

Fig. 7. Integral equations for the ground state energy in terms of two-particle functions A(k) (fig.7a) and B(k) (fig.7b). The shadowed areas are vertices. The first terms are lowest order two-particle functions. The coupling between different channel electrons gives the factor 3 in eq.(4.10) while the coupling between the same channel electrons gives the factor 1.

Fig. 8. The selfenergy of the unoccupied state as a function of z at zero temperature. Only the part below $2\varepsilon_f - I$ is drawn. z is in units of T_k. The constant $2\varepsilon_f - I$ is taken to be as zero on this scale for simplicity. The divergence at z=-1.26 looks like a simple pole. The solution for the ground state energy is the crossing point of function f(z)=z and function $\Sigma_0(z)$. The parameters are chosen to be : $\varepsilon_f = -6.5$, $\rho V^2 = 1.0$, $D = 22.22$, $I = 0.3$ and $T_k = D \exp(-\frac{1}{\varepsilon_f}) = 0.0334$.

List of Tables

Chapter 1 : Introduction

The physical properties of the Kondo and the mixed valence systems have long been of great interest and a challenge to condensed matter theorists in the past two decades (1-8). The discovery of the heavy Fermion superconductors (4,9,10,11) recently has generated a great deal of new interest on the problem since these heavy fermion compounds have shown similar characteristic behaviors to that of dilute and concentrated Kondo systems.

1.1 Single Impurity Kondo Problem

Many rare earth alloy systems have anomalous but similar properties at low temperatures. In these systems the rare earth ions are embedded in a continum of a delocalized electron band and interact with the conduction electrons. It is generally believed that these systems can be described by the degenerate Anderson model. The Anderson model contains much richer structure than the original Kondo model but they are equivalent

via a canonical transformation (5) if the parameters are chosen properly. The main difficulty in solving the Kondo problem is the infrared divergence (6,7) associated with the physical quantities. For example : the magnetic susceptibility calculated perturbatively has an expansion form :

$$\frac{\chi}{g\mu_B^2} = \rho \frac{J}{T} \left(1 + \rho J \log T/D + (\rho J \log T/D)^2 + \cdots \right)$$

At the temperature

$$T = T_k = De^{\frac{1}{\rho J}}$$

all terms in the perturbation series are of order 1 and the perturbation approximation breaks down. This instability prevents one from using the usual perturbative techniques at lower temperatures.

In order to overcome this difficulty , nonperturbative methods such as the numerical renormalization group (7) and Bethe Ansatz (8) have been developed successfully and the exact ground-state solution has been found in one dimension. Since these two methods are very difficult to extend to the concentrated systems the perturbative diagrammatical method has been intensively studied in recent years.(12-15) The famous 1/N expansion proposed by Ramakrishnan and Anderson (16) has been applied to the Anderson model by numerous groups (10,11,12) and the best results are in excellent agreement with the exact solutions.

The distinctive physics of the Kondo problem is the spin flip scattering of conduction electrons by the impurity. Due to this scattering the impurity spin is compensated by the conduction electons at a characteristic temperature T_k to form a singlet. This is known

as the Kondo screening effect. The Kondo temperature T_k is the characteristic energy which determines all of the important physical properties of the system.

1.2 Heavy Fermion Superconductors and The Concentrated Kondo Problem

A few years ago a group of rare earth compounds were found to be superconducting at very low temperatures with very unusual properties. These compounds are called heavy fermion superconductors (HFSC). The characteristic of the HFSC is the anomalous electron effective mass of $10^2 - 10^3$ times that of the free electron. This is manifested in the specific heat measurement at low temperatures. The large specific heat corresponds to the high density of states at Fermi level which is generally attributed to the effect known as Kondo resonance. While the HFSC systems show a single characteristic energy scale just as in the dilute magnetic impurity systems there is also a clear coherent effect in the resistivity measurements which is believed to come from impurity-impurity interactions. The problem of explaining this unusual phenomenon has generated new interest in the dilute and concentrated Kondo systems for both theorists and experimentalists.

Since the properties of the dilute impurity system are well understood, a lot of effort has been spent on the concentrated systems in the past few years.(12,14,15,17) Unlike dilute impurity systems where the interactions between the impurities can be neglected one has to consider these intersite interactions between impurities. These intersite interactions can sometimes be very important and change the whole physical picture. In the lattice

case, for example, coherent scattering has to be accounted for and is believed to cause the low temperature resistivity to differ so much from that of dilute systems.

Due to the mathematical difficulties in solving the lattice model the system with just two impurities is of great interest because it contains the simplest and most important inter-site interaction known as Ruderman-Kittel-Kasuya-Yosida (RKKY) interaction. The interplay between the RKKY interaction and the Kondo effect can give one a great deal of insight into the difference between the dilute and concentrated systems.

Jayaprakash et al.(17) have done pioneer work on the two-impurity Kondo problem by using the thermodynamic scaling method. The main conclusion is that in the limit that the RKKY interaction is larger than the Kondo temperature there will be a two-stage Kondo effect and two corresponding energy scales. Rasul and Hewson (14) have calculated the lowest order intersite contributions to the ground state energy. Abraham and Varma (19) also calculated intersite terms diagrammatically and pointed to the possible existence of a new divergence.

In our article we will use the diagrammatical method developed by Keiter and Kimball and Grewer and Keiter (12) to do the calculations on the high temperature magnetic susceptibility perturbatively and to do infinite order summation for the ground state energy. Also we will compare our results with other groups.

1.3 The Organization of The Dissertation

The dissertation is organized as follows: In chapter 2 we will outline the formal theories of the Feynman and Goldstone diagram approach to the Anderson model. We will first perform a canonical transformation to the two-impurity Anderson model and write the Hamiltonian in terms of projection operators. The diagrammatical rules can then be derived from the time ordered perturbative expansion method. In chapter 3 we will examine the high temperature limit perturbatively through the magnetic susceptibility calculations in different regimes. The results will be compared with the scaling theory result. We will derive and solve the self energy equations at high temperature to obtain two Kondo temperatures in chapter 4. The integral equations for the ground state energy will also be derived and solved numerically. Some variational calculations will be done to verify our results. The conclusions will be given in chapter 5.

Chapter 2: The Formal Theory of the Perturbative Diagrammatical Method

2.1 The Anderson Hamiltonian

The Hamiltonian describing a system in which magnetic impurities located on a lattice interact with a continuum of conduction electrons can be written in the following form, known as the Anderson model:

$$H = H_0 + H_{mix}$$

$$H_0 = \sum_{\vec{k}m} \varepsilon_{\vec{k}m} C^{\pm}_{\vec{k}m} C_{\vec{k}m} + \sum_{lm} \varepsilon_{fm} f^{+}_{lm} f_{lm} + \frac{U}{2} \sum_{l,n,m\neq n} f^{+}_{lm} f_{lm} f^{+}_{ln} f_{ln} \qquad (2.1a)$$

$$H_{mix} = \sum_{\vec{i}\vec{k}m} [V_{\vec{k}m} C^{\pm}_{\vec{k}m} f_{im} e^{(\vec{ik} \cdot \vec{r}_i)} + H.C.] \qquad (2.1b)$$

where $\vec{r}_i$'s are the positions of impurities located on a lattice, m and n are the magnetic qauntum numbers and $\vec{k}$ is the conduction band wave vector. $C^{\pm}_{\vec{k}m}(C_{\vec{k}m})$ is a creation (annihilation) operator for the conduction electrons and $f^{\dagger}_{im}(f_{im})$ is a creation (annihilation) operator for an impurity at site i . $\varepsilon_{\vec{k}}$ is the conduction electron energy in the range $-D < \varepsilon_{\vec{k}} < D$ where D is the band width of a half filled band. The band is assumed to be S-like which means that no orbital degeneracy will be considered. ε_{fm} is the energy difference between the occupied and unoccupied f state. U is the strong coulomb repulsive energy which we will take to be infinitely large. This will prevent the f-state on each site from being doubly occupied. H_{mix} describes the mixing of strength V between the localized f states and the conduction electrons. We will be working in the configuration in which the H_0 part of the Hamiltonian is diagonalized and we will treat the H_{mix} part as perturbation.

As indicated before, the difference between the lattice and the single impurity model is the intersite interaction induced by the hybridization H_{mix}. The simplest Hamiltonian that can produce this interaction is the two-impurity model. In the limit $U \to \infty$ the two impurity Anderson model with the impurities located at $\pm \vec{r}/2$ can be written in the following form :

$$H = H_0 + H_1$$

$$H_0 = \sum_{\vec{k}m} \varepsilon_{\vec{k}m} C^{\pm}_{\vec{k}m} C_{\vec{k}m} + \sum_{m} \varepsilon_{fm} (n_{1fm} + n_{2fm})$$

$$H_1 = \sum_{\vec{k}m} [(V_{\vec{k}m} C^{\pm}_{\vec{k}m} (f_{1m} \exp^{(i\frac{\vec{k}\cdot\vec{r}}{2})} + f_{2m} \exp^{(-i\frac{\vec{k}\cdot\vec{r}}{2})})) + H.C.] \tag{2.2}$$

$V_{\vec{k}m}$ varies very slowly as a function of $\vec{k}$ and m we can neglect its k vector and m dependence. This will simplify calculations considerablely while having no significant effect on the final results.

Furthermore it is more convenient to study the two-impurity Anderson model in certain regimes by defining two orthogonal conduction electron channels as well as two f electron operators which are even and odd with respect to the midpoint of the impurities. We will treat impurities as spin one-half for the simplicity and the results can be generalized to the higher spin cases. Thus we define

$$a_{k\sigma} = \frac{1}{\sqrt{\lambda_+(k)}} \int \frac{d\Omega_k}{4\pi} \cos\frac{\vec{k}\cdot\vec{r}}{2} \; C_{\vec{k}\sigma} \tag{2.3a}$$

$$b_{k\sigma} = \frac{1}{\sqrt{\lambda_-(k)}} \int \frac{d\Omega_k}{4\pi} \sin\frac{\vec{k}\cdot\vec{r}}{2} \; C_{\vec{k}\sigma} \tag{2.3b}$$

where

$$\lambda_{\pm}(k) = \frac{1}{2}(1 \pm \frac{\sin kr}{kr}) \tag{2.4}$$

$$f_{\frac{e\sigma}{o\sigma}} = \frac{1}{\sqrt{2}}(f_{1\sigma} \pm f_{2\sigma}) \tag{2.5}$$

$$n_{e\sigma} = f^{+}_{e\sigma} f_{e\sigma}$$

$$n_{o\sigma} = f^{+}_{o\sigma} f_{o\sigma}$$

Then the Hamiltonian becomes

$$H = \sum_{k\sigma} \varepsilon_{k\sigma}(a^{+}_{k\sigma} a_{k\sigma} + b^{+}_{k\sigma} b_{k\sigma}) + \sum_{\sigma}(n_{e\sigma} + n_{o\sigma})\varepsilon_{f\sigma}$$

$$+ \{\sum_{k\sigma} \sqrt{2}\, V_{+} a^{+}_{k\sigma} f_{e\sigma} + \sum_{k\sigma} \sqrt{2}\, V_{-} b^{+}_{k\sigma} f_{o\sigma} + H.C.\} \tag{2.6}$$

where

$$V_{\pm}(k) = \sqrt{\lambda_{\pm}(k)}\; V = \sqrt{\frac{1}{2}(1 \pm \frac{\sin kr}{kr})}\, V \tag{2.7}$$

The unperturbed basis states are :

$$| \Phi > = | 0 >$$

$$| e\sigma > = \frac{1}{\sqrt{2}} (f^{+}_{1\sigma} + f^{+}_{2\sigma}) | \Phi >$$

$$| o\sigma > = \frac{1}{\sqrt{2}} (f^{+}_{1\sigma} - f^{+}_{2\sigma}) | \Phi >$$

$$| 2\sigma > = f^{+}_{1\sigma} f^{+}_{2\sigma} | \Phi > \qquad (2.8)$$

$$| 2e > = \frac{1}{\sqrt{2}} (f^{+}_{1\uparrow} f^{+}_{2\downarrow} + f^{+}_{1\downarrow} f^{+}_{2\uparrow}) | \Phi >$$

$$| 2o > = \frac{1}{\sqrt{2}} (f^{+}_{1\uparrow} f^{+}_{2\downarrow} - f^{+}_{1\downarrow} f^{+}_{2\uparrow}) | \Phi >$$

where the state $| \Phi >$ is unoccupied by the f electrons (f_0), states $| e\sigma >$ and $| o\sigma >$ are singly occupied (f_1) and the states $| 2\sigma >$, $| 2e >$ and $| 2o >$ are doubly occupied (f_2) We can see now that the Hamiltonian (2.6) contains two one-dimensional conduction electron bands A and B. The summation with respect to the solid angle of $\vec{k}$ has been performed in the definitions of new operators. The conduction and the f electron operators and basis states are now all defined as even or odd instead of being labelled with site 1 and 2.

In terms of projection operators the mixing part of the Hamiltonian can be written as :

$$H_1 = \{ \sum_{k\sigma} \sqrt{2}\, V_{+} a^{+}_{k\sigma} [\, | \Phi >< e\sigma | \; - | o\sigma >< 2\sigma | - \frac{1}{\sqrt{2}} | o - \sigma >< 2e |$$

$$+ \frac{\sigma}{\sqrt{2}} | e - \sigma >< 2o |] \} + \{H.C.\}$$

$$+ \{ \sum_{k\sigma} \sqrt{2}\, V_{-} b^{+}_{k\sigma} [\, | \Phi >< o\sigma | + | e\sigma >< 2\sigma | \; + \frac{1}{\sqrt{2}} | e - \sigma >< 2o |$$

$$-\frac{\sigma}{\sqrt{2}} \mid o-\sigma><2e\mid]\} + \{H.C.\} \qquad (2.9)$$

We can see that each term in the Hamiltonian (2.9) lowers the f state occupation number by one by creating either an A channel or a B channel conduction electron. The Hermitian conjugate part of the Hamiltonian represents the inverse processes. These processes are the elementary excitations of the system. The diagrams we are going to use are just a representation of these excitations. The Hamiltonian has many terms with different coefficients and the Feynman rules will be much more complicated than the ones in the single impurity case.

2.2 The Feynman-Goldstone Diagrams for the Two-Impurity Anderson Hamiltonian

The perturbative diagrammatic method which we are going to use was first developed by Keiter and Kimball and by Grewe and Keiter (12) and later revised by Lee and Zhang (13). The diagrammatic rules can be obtained by doing the perturbative expansion formally and calculating all possible contractions of time ordered operators of both conduction and f electrons. We do not intend to go through the derivation procedure in detail here since it is rather tedious. We will only summarize the final rules. There are two ways to classify the diagrams for the two-impurity Anderson model. One way is to arrange the interaction terms according to the sites. Each site has its own time ordering

or its complex frequency. The onsite interactions are treated on the same footing as in the single impurity case. Then the onsite Feynman-Goldstone diagrams on different sites are connected via the band Green's functions. This method has fewer number of diagrams and it is easier to identify the diagrams with the physical processes. The results in section 3.3 are obtained with this method. It is more convenient to do this when one wants to do the finite order intersite calculation while including the onsite self energies. However, if we want to sum the intersite terms to infinite order this method becomes very inconvenient since the intersite terms contain more than one complex variable and it is very difficult to write them as self energies. The second way is to use only one time ordering parameter i.e one complex frequency, so that we can treat the intersite terms in the same way we treat the onsite terms. The price we pay is that there are more diagrams and each diagram may not correspond to an identifiable physical process. The major part of our calculation is done in second way. Thus we will give diagram rules for this method only. The diagram rules of the first method can be found in ref. (12).

The diagram rules can be summarized as follows :

For a diagram which is 2n-th order in $V_{\pm}$, draw a dashed vertical line and distribute 2n interacton vertices on it. Specify the initial state and its occupation probability. Represent a singly occupied state f_1 by a wiggly line , a doubly occupied state f_2 by a double wiggly line and an unoccupied state f_0 by blank. Distribute these lines between the vertices in all possible ways. Each vertex changes the f electron occupation number by one and only one. Connect all vertices by either an A channel or a B channel conduction electron each represented by a full line labeled by a or b respectively. All full lines have directions attached to them. Each descending (ascending) A [B] channel line contributes a fermi statistical factor $f_{k\sigma}(1-f_{k\sigma})$ and a matrix element $V_{\mp}^2$ [$V_{\pm}^2$]. Each

vertex can have only one full line entering or leaving it. Each full line carries an energy $\varepsilon_{k\sigma}$ and each wiggly line an energy $\varepsilon_{f\sigma}$. When doing this we have to take the Pauli exclusion principle into account, i.e. no two electron lines from the same channel with the same spin enter two successive vertices. Furthemore, a vertex involving the states f_0 or f_2 contributes a factor $\sqrt{2}$. The contribution from the diagram to the partition function is given by :

$$I = \frac{1}{2\pi i} \int_C dz e^{-\beta z} \prod_{l=0}^{n-1} \frac{1}{z - \varepsilon_l} \tag{2.10}$$

where ε_l is the excitation after the i-th vertex calculated by subtracting the energies of outgoing lines and adding the energies of incoming lines. C encloses all poles of the integrand. The sign of a diagram can be determined as follows : a) each crossing of the full lines gives a negative sign; b) the vertices involving an A channel electron and doubly occupied states each give a negative sign: c) the vertices involving the state $|2o>$ and conduction electrons with down spin each contribute an extra negative sign. Finally the product is taken over the initial occupation probability, the matrix elements, the integral and the Fermi factors and the summation is performed over all initial and internal f and conduction electron quantum numbers. For an illustration of the rules two diagrams are drawn in figure 1 and the self-energy value of each diagram is given below :

$$\Sigma_{2a}(z) = \sum_k \frac{V_+^2 f_k}{z + \varepsilon_k - \varepsilon_{f\sigma}} \tag{2.11a}$$

$$\Sigma_{2b}(z) = \sum_{kk'} \frac{(-1)^2 4 V_+^2 V_-^2 (1-f_k)(1-f_{k'})}{(z+\varepsilon_{f\sigma}-\varepsilon_k)(z+2\varepsilon_{f\sigma}-\varepsilon_k-\varepsilon_{k'})(z+\varepsilon_{f\sigma}-\varepsilon_{k'})} \tag{2.11b}$$

Chapter 3 : The High Temperature Perturbative Result

3.1 The Motivation and the Model Hamiltonian

The problem of the two-impurity Kondo system had only been studied by a few groups because of its difficulty (14,15,17). Five years ago Jayaprakash et al. (17) used a generalized poor man's scaling method (4) to study this model. They have given a very interesting conclusion that in the limit where the RKKY interaction I is much larger than the Kondo temperature there is a two-stage Kondo effect and the ground state is a spin singlet formed from the screened impurity spin triplet. Recently Abraham and Varma (19) have reported (in contradiction to the results of Jayaprakash et al.) a possible new divergence from the intersite interaction in the perturbative calculation of the two-impurity model. They claim that the two impurities will pair up coherently no matter how small the initial RKKY interaction is. This controversy has brought the need for a careful examination of the perturbative expansion to the attention of the theoretical

community. In this chapter we will derive the magnetic susceptibility to fourth order in the coupling constant J for three different regimes. In the first regime we assume that the temperature is greater than all the relevant interactions. In this regime we have found the well known divergent terms due to the Kondo effect. One of these terms is the one pointed out by Abraham and Varma. Depending on the ratio of the two relevant energy scales $\frac{T_k}{|I|}$, we will have two different ways to introduce the renormalization as temperature lowers. In the regime where T_k is greater than $|I|$ and the temperature T, we have recalculated the magnetic susceptibility by including the Kondo screening in the self energy. The susceptibility then has no divergent terms at low temperatures as the magnetic moments are quenched. The most interesting regime occurs when $|I|$ is greater than T_k and the temperature T. To make the perturbation calculation more efficient we transform the conduction electrons into even and odd states with respect to the midpoint of the impurities as discussed above. The Hamiltonian is then written in terms of the total spin of the impurities. The magnetic susceptibility is calculated by treating I as a self energy for both cases of I being positive or negative.

As indicated before, the Anderson Hamiltonian in the Kondo regime, i.e. $-\varepsilon_f >> \rho V^2$, has the same behavior as the Kondo exchange model. Making the Schrieffer-Wolff transformation (1) to the two-impurity Anderson Hamiltonian of eq. (2.2) we obtain the two-impurity Kondo Hamiltonian

$$H_{2K} = \sum_{\vec{k}\sigma} \varepsilon_{\vec{k}\sigma} n_{\vec{k}\sigma} - \frac{J}{2} \sum_{i=1}^{2} (S_i^+ \sigma_i^- + S_i^- \sigma_i^+) - \frac{J}{2} \sum_{i=1\sigma}^{2} \rho_{i\sigma} n_{i\sigma} \tag{3.1}$$

where $J = \frac{2V^2}{\varepsilon_f} < 0$. The spin and the density fluctuation operators are given by

$$S_l^{+(-)} = f_{l\uparrow(\downarrow)}^{+} f_{l\downarrow(\uparrow)} \tag{3.2}$$

$$\sigma_l^{+(-)} = \sum_{\vec{k}\vec{k}'} e^{i(\vec{k}-\vec{k}')\cdot\vec{R}_l} C_{\vec{k}\uparrow(\downarrow)}^{\pm} C_{\vec{k}'\downarrow(\uparrow)} \tag{3.3}$$

$$\rho_{l\sigma} = \sum_{\vec{k}\vec{k}'} e^{i(\vec{k}-\vec{k}')\cdot\vec{R}_l} C_{\vec{k}\sigma}^{\pm} C_{\vec{k}'\sigma} \tag{3.4}$$

Here we have neglected the f electron hopping term but retained the potential scattering term which we include in the third term in eq. (3.1). This is the only difference between our model and the model studied by Jayaprakash et al. It is well known that the potential scattering terms do not change the low temperature properties of the Kondo systems, so the outcomes from the two models should be the same. The magnetic susceptibility for the Hamiltonian H_{2K} will be calculated by using the Goldstone diagrammatic method devoloped by Keiter et al. (9) and revised by Lee and Zhang (10).

3.2 The High Temperature Regime

The magnetic susceptibility due to impurities is calculated in a straightforward perturbative expansion. This expansion is valid only in the high temperature regime. For convenience of discussion we shall separate the results into three parts, i.e.

$$\frac{T\chi}{g^2\mu_B^2} = \frac{2}{4} + T\chi_1 + T\chi_2 + T\chi_3 \tag{3.5}$$

Here χ_1 involves only the on-site processes, χ_2 includes contributions from intersite potential scattering and on-site spin flip terms, and χ_3 represents a new process involving the spin flip scatterings on both sites while electrons are exchanged. In our calculaton we will always neglect terms of order $\ln \varepsilon_f/D$ because ε_f and D are of the same order. The leading and the next leading logarithmically divergent terms obtained for one impurity are given by

$$T\chi_1 = \frac{2}{4}\rho J[1 + y + y^2 + y^3 + \rho J(7/4 + 4y + \frac{13}{2} Y^2)] \tag{3.6}$$

where

$$y = \rho J \ln T/D \tag{3.7}$$

and ρ is the density of states at the fermi level which is assumed to be constant. This result agrees with the perturbative result given by Wilson (3) and other groups. The second term for the susceptibility χ_2 is given by

$$T\chi_2 = \frac{1}{4}\{\frac{I}{2T} + (\rho J)^2 \pi \frac{\sin 2\alpha}{\alpha^2} y\} \tag{3.8}$$

where

$$\alpha = k_F R$$

and I is the famous RKKY interaction, given by

$$I = J^2 \sum_{kk'} \frac{f_k(1-f_{k'})}{\varepsilon_k - \varepsilon_{k'}} \; e^{i(\vec{k}-\vec{k}')\cdot\vec{R}} \cong \frac{\pi}{4}(\rho J)^2 \; \frac{\cos 2\alpha}{\alpha^3} \tag{3.9}$$

in the limit of large $k_F R$ (12). The first term in eq. (3.8) is from the lowest order intersite interaction. Its proportionality to 1/T suggests this term is the lowest order intersite self-energy. The logarithmic divergence in the second term is essentially from the renormalization effect of Kondo screening on the intersite interactions. This will become clearer later on. The third term, χ_3, represents a purely intersite term first obtained by Abraham and Varma (16), given by

$$T\chi_3 = \frac{I}{4T} \; (\rho J)^2 \left(\frac{\sin\alpha}{\alpha}\right)^2 \; \ln(D/T) \tag{3.10}$$

At first glance it seems that this divergent term will result in a new energy scale at which the intersite interaction becomes infinite and the two-impurity pairing will become inevitable. However, since the energy scale associated with this divergence is much smaller than the Kondo temperature, we have to consider the renormalization effect of other interactions, i.e. we must recalculate this term by taking either Kondo screening or RKKY interaction as selfenergy. We will see that this divergence disappears and the important energy scales are still T_k and I.

3.3 Kondo Temperature Larger than RKKY Interaction

In the regime where $T_k > |I|$ and T, we use Kondo screening selfenergy in just the order of the leading 1/N expansion for simplicity to renormalize the intersite coupling. The result is that the magnetic moments of the impurities are quenched at temperature $T_k = D \exp^{\frac{-1}{\rho J}}$ and there are no longer any divergent terms left since the intersite coupling or the RKKY interaction is now strongly renormalized due to the moment-quenching. As a consequence the magnetic susceptibility for the single impurity is proportional to $\frac{1}{T_k}$ (3). The contribution from leading intersite coupling terms to the susceptibility $\chi'_2 + \chi'_3$ gives us

$$\chi'_2 = -\frac{\pi}{8} \frac{\sin 2\alpha}{\alpha^2} \frac{1}{T_k} \tag{3.11}$$

$$\chi'_3 = \frac{1}{4} \left(\frac{\sin \alpha}{\alpha}\right)^2 \frac{I}{T_k^2} \tag{3.12}$$

Eq. (3.11) was first derived by Rasul and Hewson (14). Notice that the Kondo temperature T_k is now effectively cutoff energy. The new intersite contribution χ'_2 is essentially due to the overlapping of the wave functions of the conduction electrons participating in screening the two Kondo impurities. The divergent term in eq. (3.9) is now quenched by the Kondo screening and the system can be described as two screened Kondo singlets with a weak residual interaction. They are not likely to pair up in the ground state.

3.4 RKKY Interaction Larger than Kondo Temperature

In the limit that the RKKY interacton has much greater influence than the Kondo effect, the two impurities will pair up and behave either like a spin-one triplet or spin-zero singlet depending on whether I is positive or negative. If I < 0 , the total spin S = 0 state (singlet) has lower energy (by an amount -I) than the S = 1 (triplet) state. At temperature T << -I the two impurities will be locked up antiferromagnetically to form an effective spin-zero singlet and no Kondo screening will occur. In this case the susceptibility can be calculated by a second order perturbation theory easily . If I > T_k and temperature, we will have an effectively S = 1 Kondo problem. The divergent terms discussed by Abraham and Varma once again are renormalized away after we take the RKKY interacton as self energy. The divergent terms left are all due to the Kondo effect. In this limit we will choose the triplet and singlet states of the total spin operator $\vec{S} = \vec{S}_1 + \vec{S}_2$ as the basis states for the sake of convenience. Performing a canonical transformation on the Hamiltonian (3.1) as we did in chapter 2, we have

$$H_{2k} = \sum_{k\sigma} \varepsilon_{k\sigma}(a^+_{k\sigma}a_{k\sigma} + b^2_{k\sigma}b_{k\sigma}) + 2\sum_{\sigma} \varepsilon_{f\sigma}n_\sigma$$

$$- \sum_{kk'} \frac{J_+(kk')}{\sqrt{2}} (S^+\sigma^-_a + S^-\sigma^+_a) - \sum_{kk'} \frac{J_-(kk')}{\sqrt{2}} (S^+\sigma^-_b + S^-\sigma^+_b)$$

$$+\sum_{kk'}\frac{J_{+-}(kk')}{\sqrt{2}}\,(S_0^+\sigma_{ab}^- + S_0^-\sigma_{ab}^+) - \sum_{\sigma kk'} J_+(kk')n_\sigma\rho_{a\sigma}$$

$$-\sum_{\sigma kk'} J_-(kk')n_\sigma\rho_{b\sigma} + \sum_{\sigma kk'} J_{+-}(kk')n_{0\sigma}\rho_{ab\sigma} \tag{3.13}$$

where a_k and b_k are defined as in chapter 2 and

$$J_\pm(kk') = \sqrt{\lambda_\pm(k)\lambda_\pm(k')}\,J \cong \lambda_\pm(k_F)J \tag{3.14a}$$

$$J_{+-}(kk') = \sqrt{\lambda_+(k)\lambda_-(k')}\,J \cong \sqrt{\lambda_+(k_F)\lambda_-(k_F)}\,J \tag{3.14b}$$

The operators $S^\pm$, $\sigma^\pm_{ab}$, etc. are defined as follows :

$$S^\pm = \frac{1}{2}(S_1^\pm + S_2^\pm)$$

$$\sigma_a^+ = a_{k\uparrow}^+ a_{k'\downarrow}$$

$$\sigma_{ab}^+ = a_{k\uparrow}^+ b_{k'\downarrow} + b_{k'\uparrow}^+ a_{k\downarrow}$$

$$\rho_{ab\sigma} = a_{k\sigma}^+ b_{k'\sigma} + b_{k'\sigma}^+ a_{k\sigma}$$

$$\vec{S}_0 = \frac{1}{2}(\vec{S}_1 - \vec{S}_2)$$

$$n_\sigma = \frac{1}{2}(n_{1\sigma} + n_{2\sigma})$$

and

$$n_{0\sigma} = \frac{1}{2}(n_{1\sigma} - n_{2\sigma})$$

The structure of the transformed Hamiltonian shows that there are two one-dimensional conduction electron bands (a and b) coupling to the S = 1 and S = 0 impurity states with the strength J_+ and J_- respectively. These coplings do not change the total spin S of the impurities. The transition between the singlet and the triplet is represented by the interaction between the bands with the strength J_{+-}. Now we effectively have only one impurity with complicated internal degrees of freedom. The diagrammatic technique of the single impurity Anderson model can now be applied. The self-energies due to the lowest order intersite interaction for the triplet and the singlet are I/2 and -I/2 respectively. Thus by taking into account these self-energies the triplet splits away from the singlet. Transitions from the singlet to the triplet require an energy I. Therefore, in the temperature range $T_K << T << I$, each triplet has occupation probability 1/3 while the singlet has zero. Hence we only need to consider those diagrams with the triplet as initial and final states. The magnetic susceptibility obtained is separated into two parts, i.e.,

$$\frac{T\chi}{g^2\mu_B^2} = \frac{2}{3} + T\chi''_1 + T\chi''_2 \tag{3.15}$$

The constant 2/3 is due to the fact that only two out of three states in the triplet have magnetic moment. The second part of susceptibility is given by

$$T\chi''_1 = \frac{2}{3}\{\rho J_+[1 + Y_+ + Y_+^2 + Y_+^3] + \rho J_-[1 + Y_- + Y_-^2 + Y_-^3]\} \tag{3.16}$$

where

$$Y_{\pm} = \rho J_{\pm} \ln T/D + \rho J_{\mp} \ln I/D. \tag{3.17}$$

Here we have listed only the leading divergent terms in χ_1''. It is straightforward to show that in the limit $\alpha = k_F R \to \infty$ the leading divergent terms in eq. (3.6) are identical to those in $T\chi''_1$ given above. Thus χ''_1 represents the usual Kondo spin-flip scattering between a S = 1 impurity and two conduction electron channels with two coupling constants J_+ and J_-. The series of Y_+ and Y_- in eq. (3.16) will lead to two energy scales T_{k+} and T_{k-}. Their values are determined by the equations $Y_{\pm}(T_{k\pm}) = 1$. Explicitly, they are of the form :

$$T_{k\pm} = I \exp \frac{\ln D/I + \dfrac{1}{\rho J}}{\lambda_{\pm}(k_F)} = I \left(\frac{T_k}{I}\right)^{\frac{1}{\lambda_{\pm}}} \tag{3.18}$$

These results are in complete agreement with those of the scaling theory (10). The pure intersite contribution in χ_2 of equation (3.8) is essentially the same as what we obtain for χ_2'', given by

$$T\chi_2'' = \frac{\pi}{3} (\rho J)^2 \frac{\sin 2\alpha}{\alpha^2} \; Y \tag{3.19}$$

As compared to χ_2 of eq. (3.8), the renormalization by the RKKY interacton only changes the number of degenerate states from 4 to 3 in χ_2''. The divergent term χ_3 in eq. (3.10), also obtained by Abraham and Varma, has once again been renormalized away as suggested (to the cogniscenti) by its proportionality to I.

Chapter 4 : The Self Energies and the Ground State

4.1 The Unperturbed States

Using the Kondo Hamiltonian is easier when one wants to do high temperature calculations and examine the temperature dependence of physical quantities qualitatively. However, if one wants to study the low temperature behaviour of the dilute and concentrated impurity systems quantitatively the Anderson Hamiltonian would be more convenient and gives more information about the physical properties of the system due to its richness in structure. That is why we are going to use the Anderson Hamiltonian in our self energy calculation in this chapter.

As discussed in chapter 2 the unperturbed eigenstates of the two-impurity Anderson Hamiltonian contain one unoccupied (f_0), 4 singly occupied (f_1) and 4 doubly occupied (f_2) magnetic states in the conduction electron Fermi sea. (see fig. 2.) The energy of the f_0 state is the fermi energy which is taken to be zero. The states f_1 and f_2 have energies ε_f and $2\varepsilon_f$ relative to the fermi energy respectively. In the Kondo regime the magnetic

states are very deep in the fermi sea so that they are always occupied in the absence of the perturbation. Furthermore the energy of the f states ε_f has a very large negative value that satisfies the condition $-\varepsilon_f >> \Delta$, where $\Delta = \rho V^2$ is the characteristic transition strength between the magnetic states and ρ the density of states at Fermi energy. Thus at temperature $T < -\varepsilon_f$ the magnetic states are still occupied. However, due to the strong temperature dependence of the hybridization we could have cross-overs between the various states at some temperature. We are going to examine this possibility through the self energy calculation below.

In the single impurity Anderson model it has been shown (13) that the crossed diagrams have little contribution to the ground state energy so that one can get two coupled integral equations for the occupied and unoccupied states after neglecting the crossed diagrams. However this is not the case with the two-impurity model; the crossed diagrams are important, in fact they can be leading order diagrams as far as the 1/N expanson is concerned. Therefore we must be careful throughout the self energy calculation in determining whether a crossed diagram should be kept or thrown away.

Following the diagrammatical rules in chapter 2 we can draw the non-crossing part of the Dyson self energy diagrams easily as shown in figure 3. The integral equations for these diagrams are written down below along with the formal crossed diagram contribution :

$$\Sigma_0(z) = \sum_{k\sigma} \frac{2V_+^2 f_k}{z + \varepsilon_k - \varepsilon_\sigma - \Sigma_{e\sigma}} + \sum_{k\sigma} \frac{2V_-^2 f_k}{z + \varepsilon_k - \varepsilon_\sigma - \Sigma_{o\sigma}} + \Sigma_0^c(z) \qquad (4.1a)$$

$$\Sigma_{e\sigma}(z) = \sum_k \frac{2V_+^2(1-f_k)}{z-\varepsilon_k+\varepsilon_\sigma-\Sigma_0} + \sum_k \frac{2V_-^2 f_k}{z+\varepsilon_k-\varepsilon_\sigma-\Sigma_{2\sigma}}$$

$$+ \sum_k \frac{V_-^2 f_k}{z+\varepsilon_k-\varepsilon_{-\sigma}-\Sigma_{2e}} + \sum_k \frac{V_+^2 f_k}{z+\varepsilon_k-\varepsilon_{-\sigma}-\Sigma_{2o}} + \Sigma_{e\sigma}^c(z) \qquad (4.1b)$$

$$\Sigma_{o\sigma}(z) = \sum_k \frac{2V_-^2(1-f_k)}{z-\varepsilon_k+\varepsilon_\sigma-\Sigma_0} + \sum_k \frac{2V_+^2 f_k}{z+\varepsilon_k-\varepsilon_\sigma-\Sigma_{2\sigma}}$$

$$+ \sum_k \frac{V_+^2 f_k}{z+\varepsilon_k-\varepsilon_{-\sigma}-\Sigma_{2e}} + \sum_k \frac{V_-^2 f_k}{z+\varepsilon_k-\varepsilon_{-\sigma}-\Sigma_{2o}} + \Sigma_{o\sigma}^c(z) \qquad (4.1c)$$

$$\Sigma_{2\sigma}(z) = \sum_k \frac{2V_-^2(1-f_k)}{z-\varepsilon_k+\varepsilon_\sigma-\Sigma_{e\sigma}} + \sum_k \frac{2V_+^2(1-f_k)}{z-\varepsilon_k+\varepsilon_\sigma-\Sigma_{o\sigma}} + \Sigma_{2\sigma}^c(z) \qquad (4.1d)$$

$$\Sigma_{2e}(z) = \sum_{k\sigma} \frac{V_-^2(1-f_k)}{z-\varepsilon_k+\varepsilon_\sigma-\Sigma_{e\sigma}} + \sum_{k\sigma} \frac{V_+^2(1-f_k)}{z-\varepsilon_k+\varepsilon_\sigma-\Sigma_{o\sigma}} + \Sigma_{2e}^c(z) \tag{4.1e}$$

$$\Sigma_{2o}(z) = \sum_{k\sigma} \frac{V_+^2(1-f_k)}{z-\varepsilon_k+\varepsilon_\sigma-\Sigma_{e\sigma}} + \sum_{k\sigma} \frac{V_-^2(1-f_k)}{z-\varepsilon_k+\varepsilon_\sigma-\Sigma_{o\sigma}} + \Sigma_{2o}^c(z) \tag{4.1f}$$

where the superindices c stand for crossing.

The energy level of each state now can be determined by solving the self energy equations

$$z_0 - \Sigma(z_0) = 0 \tag{4.2}$$

where the self energy $\Sigma(z)$ can be any of the self energies in eqs. (4.1). Here we have included all the irreducible non-crossing diagrams. We don't give the expressions for the crossed diagrams because they are very complicated. Some examples have been given in figure 4 which are important to the lowest order intersite interactions and to the magnetic susceptibility as shown in Chapter 3.

4.2 High Temperature Results and The first Kondo Temperature

At high temperatures the doubly occupied states have lowest energy. The fluctuations between the f_0, f_1 and f_2 will make the energy levels of all these states shift downwards with different rates as the temperature is lowered. If we only consider the second order self energies we will get exactly same results as in the single impurity case since I comes into play only in 4th or higher orders. At temperature $T \cong T_k$ the state f_0 will cross both f_1 and f_2 states and acquire a lower energy. This is the well known Kondo screening effect. This is only natural because we did not consider the intersite interactions which only come in at or above 4th order in V.

As discussed before we have to include the crossed diagrams when we calculate the high orderer diagrams. The direct calculation in chapter 3 has shown in eq. (3.16) that the contribution to the magnetic susceptibility from the crossed diagrams has leading order logarithmic divergences. These crossed diagrams exist in all orders in V^2 and their contributions to the self energies can be obtained in forms of vertex functions. The vertex functions satisfy certain integral equations themselves. A diagrammatic example is shown in figure 5. The integral equations are very complicated and very difficult to solve. However there is a way to avoid calculating these vertex integral equations directly. First if we expand the selfenergies of eq. (4.1d-f) to the fourth order in $V_\pm$ for the f_2 states and separate the Kondo screening terms from the intersite terms we will get

$$\Sigma_{2\sigma} = \Sigma_{2e} = \sum_k \frac{2V_-^2(1-f_k)}{z-\varepsilon_k+\varepsilon_\sigma} + \sum_k \frac{2V_+^2(1-f_k)}{z-\varepsilon_k+\varepsilon_\sigma} - \frac{I}{2} \tag{4.3a}$$

$$\Sigma_{2o} = \sum_k \frac{2V_+^2(1-f_k)}{z-\varepsilon_k+\varepsilon_\sigma} + \sum_k \frac{2V_-^2(1-f_k)}{z-\varepsilon_k+\varepsilon_\sigma} + \frac{I}{2} \tag{4.3b}$$

where

$$I(z) = \sum_{kk'} \frac{4f_k(1-f_{k'})(V_+^2 - V_-^2)^2}{(z+\varepsilon_k-\varepsilon_\sigma)^2(z+\varepsilon_k-\varepsilon_{k'})} \tag{4.4}$$

is the RKKY interaction. We can see now that there is a difference I between the the triplet (eq. 4.3a) and the singlet (eq. 4.3b) along with an identical Kondo screening part. This interaction will cause the two impurity spins to be correlated if it is strong enough. In the limit I $>>$ T_k and when the temperature is in the range I $>>$ T $>>$ T_k ,the impurity spins will be paired ferromagnetically and the triplet has the lowest energy $2\varepsilon_f - \frac{I}{2}$. Here the renormalization part of the self energy (first two terms in eqs. (4.3)) has been combined with ε_f to form an ε_f^* (and we still call it ε_f for simplicity) while the singlet has an energy $2\varepsilon_f$ + I/2. As the temperature lowers the energy levels of the singly occupied states $e\sigma$ and $o\sigma$ will shift downwards with different rates and eventually will cross the triplet. The temperatures at which the crossovers happen can be determined by solving the self energy equations for the even and odd singly occupied states respec-

tively : Letting the energy of the f_1 states be equal to the that of the triplet in the eq. (2.7) we have

$$2\varepsilon_f - \frac{I}{2} - [\Sigma_{e\sigma}(2\varepsilon_f - \frac{I}{2}) + \varepsilon_f] = 0 \qquad (4.5a)$$

$$2\varepsilon_f - \frac{I}{2} - [\Sigma_{o\sigma}(2\varepsilon_f - \frac{I}{2}) + \varepsilon_f] = 0 \qquad (4.5b)$$

In order to avoid the complicated intersite vertex function in eqs. (4.5) we are going to do what we did for the f_2 states. Taking the hint from the perturbative calculation in chapter 3 we combine the potential scattering part (half of the second term in eq. (4.1b) and in eq. (4.1c)) of the self energies with the spin flip part (the third term) to eliminate the summation restrictions on the σ'. We use the result as effective self energy along with the lowest order intersite term which is - I/2 for all f_1 states. It can be shown that the rest of the noncrossing part of the self energy will effectively cancel the crossed terms through fourth order. Substituting these effective self energies into eq. (4.5) we have

$$\varepsilon_f - \sum_{k\sigma} \frac{V_-^2 f_k}{\varepsilon_k} + \sum_{k\sigma} \frac{V_+^2 f_k}{\varepsilon_k - I} = 0 \qquad (4.6a)$$

$$\varepsilon_f - \sum_{k\sigma} \frac{V_+^2 f_k}{\varepsilon_k} + \sum_{k\sigma} \frac{V_-^2 f_k}{\varepsilon_k - I} = 0 \qquad (4.6b)$$

The solutions for the eq. (4.6) are given by :

$$\varepsilon_f - 2\rho V_{\mp}^2 \ln(I/D) - 2\rho V_{\pm}^2 \ln(T_{k_\pm}/D) = 0 \tag{4.7}$$

or

$$T_{k_\pm} = I \exp^{\frac{\ln D/I + \frac{1}{\rho J}}{\lambda_\pm(k_F)}} = I(\frac{T_k}{I})^{\frac{1}{\lambda_\pm}} \tag{4.8}$$

We can see that these two Kondo temperatures are exactly the same as the results obtained in chapter 3 in eq. (3.18) The values of $T_{k\pm}$ depend on the sign and values of $\frac{\sin k_F R}{k_F R}$, which for now is assumed to be a negative number, so T_{k-} is larger than T_{k+} which means that the even states will cross the triplet first and acquire a lower energy as the temperature is lowered. This provides our second energy scale (the first is I). At this temperature the spin triplet of the combined impurities is screened by the even channel conduction electrons and becomes an effective spin one-half magnetic moment. The excitation energy of the system will have a magnitude on the order of T_{k-} below this temperature.

4.3 The Ground State Energy

For temperatures below T_{k-} one can do the perturbation calculation by taking into account the renormalization due to the first stage-Kondo effect. Then one can examine the temperature dependence of the physical quantities to get some ideas about the ground state. This calculation is rather complicated mathematically. Therefore we use another approach instead. We solve the self energy equations at zero temperature and find the

ground state energy directly. Solving equation (4.2) with the self energies of single occupied states at zero temperature we get the energies of the f_1 states E_{1e}, E_{1o} as follows:

$$E_{1e} = 2\varepsilon_f - I/2 - T_{k-} \tag{4.9a}$$

$$E_{1o} = 2\varepsilon_f - I/2 - T_{k+} \tag{4.9b}$$

They are lower than energies of the f_2 states which are $2\varepsilon_f - \frac{I}{2}$ and $2\varepsilon_f + \frac{I}{2}$ respectively. Now we only need to calculate the energy of the f_0 state and compare with that of the f_1 states to get the ground state energy. The importance of the crossed diagrams is especially manifested for the unoccupied state because they are of the leading order in 1/N, the same as the uncrossed diagrams. So here we have to keep these crossed diagrams at all times. The leading order selfenergy diagrams for the f_0 state are drawn in figure 6. These diagrams exist in all orders of V^2 and their contributions to the self energy are of the same order of magnitude. We can do the infinite order summation by using the two-particle vertex functions as do Read et al. (17). The diagrams in the Dyson equations for the vertex functions are drawn in figure 7, and these equations for the two-particle functions A and B can be expressed as integral equations as follows :

$$A(\varepsilon, z) = \frac{1}{z + \varepsilon_k - \varepsilon_\sigma - \Sigma_{e\sigma}} \left[1 + \rho V_+^2 \int_{-D}^{0} \frac{d\varepsilon' A(\varepsilon', z)}{z + \varepsilon + \varepsilon' - \frac{I}{2} - 2\varepsilon_f}\right.$$

$$\left. + 3\rho V_-^2 \int_{-D}^{0} \frac{d\varepsilon' B(\varepsilon', z)}{z + \varepsilon + \varepsilon' + \frac{I}{2} - 2\varepsilon_f}\right] \tag{4.10a}$$

$$B(\varepsilon,z)=\frac{1}{z+\varepsilon_k-\varepsilon_\sigma-\Sigma_{o\sigma}}\left[1+\rho V_-^2\int_{-D}^{0}\frac{d\varepsilon' B(\varepsilon',z)}{z+\varepsilon+\varepsilon'-\frac{I}{2}-2\varepsilon_f}\right.$$

$$\left.+3\rho V_+\sum\nolimits_+{}^2\int_{-D}^{0}\frac{d\varepsilon' A(\varepsilon',z)}{z+\varepsilon'+\varepsilon+\frac{I}{2}-2\varepsilon_f}\right] \qquad (4.10b)$$

where

$$\Sigma_{\substack{e\sigma\\ o\sigma}}(z)=3\rho V_\pm^2\int_{-D}^{0}\frac{d\varepsilon'}{z+\varepsilon_k-\varepsilon_\sigma-\frac{I}{2}}+\rho V_\mp^2\int_{-D}^{0}\frac{d\varepsilon'}{z+\varepsilon_k-\varepsilon_\sigma+\frac{I}{2}} \qquad (4.11)$$

are the leading order self energies for the f_1 states. We have changed the summations over k into the integrations over ε_k and the fermi statistical factors f_k become step functions since the temperature is zero now. We again assume a constant density of states ρ for the conduction electrons and take them out of the integrations. We use the lowest order self energies for the states f_1 and f_2, i.e. we keep the lowest order intersite terms for the states $f_2(\pm\frac{I}{2})$ and the leading order terms in 1/N for the states f_1. The external magnetic field is set to be zero. The factors of 3 in the above equations come from the transitions between states f_1 and the triplet of the f_2 states, whereas the other integral terms come from the transitions between the f_1 states and the singlet of the f_2 states naturely. Here we can see that we have two coupled integral equations coming from the coupling between the A channel and B channel conducton electrons and from inter-

actions among themselves. In the limit $R \to \infty$ the two equations in (4.7) will become the same and essentially identical to the integral equation obtained by Read et al. The uncrossed-term contributions to the self energy are only the first terms in the brackets in equations (4.10a,b) and they are small compared to the last two terms which come from the crossed diagrams. The selfenergy of the unoccupied state can be obtained easily as

$$\Sigma_0(z) = 4V_+^2 \sum_k A(z, \varepsilon_k) + 4V_-^2 \sum_k B(z, \varepsilon_k) \tag{4.12}$$

4.4 The Numerical Solution of the Ground State Energy

Attempts to solve the equations (4.10) analytically would encounter great mathematical difficulties if it is possible at all. The trial function method can be used in the limit $R \to \infty$ where $V_+ = V_- = \frac{V}{2}$ and I = 0 (14) but is not very promising in the general case. Therefore we are forced to use numerical methods for the solution. Naturally the iteration method was first used but it didn't work. The reason for this failure was that the large factors (kernels) with the A's and B's in the equations caused the iterated solutions to converge very slowly if at all. The remaining alternative is to come back to the nonperturbative matrix method. We discretized the energy ε and converted the integral equations to matrix equations. When doing this we have to be careful in choosing the discrete values of ε because the kernels are not linear functions of ε. They have maximum values at $\varepsilon = \varepsilon' = 0$ and fall off rapidly. In fact these maxima can diverge for certain values of z . The column vectors A and B also have this property. These divergences

have to be treated with great care. From the above considerations we chose the discrete ε values more densely around $\varepsilon = 0$ and cancel the positive divergences with the negative ones in the integration beforehand to reduce the error in the numerical calculation. Then the equations can be solved by the standard matrix convertion method. The solutions for the A's and B's are in the form of discrete vectors. They are calculated for various values of z so that we can find the shape of $\Sigma_0(z)$ as a function of z and thus the solution of the equation (4.12). The solutions for the ground state energy E_0 are listed in table 1 for different values of the RKKY interaction. We can see that for larger values of I the solutions differ more from the single impurity result which has the ground state energy - $2T_k$. The energies in last two rows are very close to those of scaling results which assume $I >> T_k$. A plot of Σ_0 as function of z is drawn in figure 8. The solution for the ground state energy determined by the equation $z - \Sigma_0(z) = 0$ is just the crossing point of the two functions z and $\Sigma_0(z)$.

4.5 Variational Results of Ground State

In the previous sections we have found through the selfenergy calculations that the state f_0 has lowest energy at zero temperature. Thus the ground state is a spin singlet. In order to ensure that we have included the right group of diagrams for the selfenergy we are going to do some variational calculations and compare with the diagrammatic results. It is well known that the variational calculation give upper limits for the energy levels at zero temperature. How close these energies are to the exact results heavily depend on the choice of the trial wave functions. It is just as difficult to choose an exact trial wave function as to sum all irreducible diagrams in the diagrammatic calculation. In fact

these two methods are equivalent at lowest order as can be seen below. In constructing the trial wave functions, the method we are going to use is similar to that of Varma et al. (22) . The wave function and the Hamiltonian will all be in the second quantized form. The trial wave functions will be constructed for both spin doublet and spin singlet states and the energy levels of these states will be calculated accordingly via the variational eigenvalue equations. Starting from the basis states of eq. (2.8) the trial wave functions for the doublet are constructed to be of form

$$|\Phi_D>_{e\sigma} = \alpha_0 |e\,\sigma> + \sum_k \alpha_{1k} b_{k\sigma} |2\,\sigma> + \sum_k \alpha_{2k} b_{k-\sigma} |2\,e> + \sum_k \alpha_{3k} a_{k-\sigma} |2\,o> \qquad (4.13a)$$

$$|\Phi_D>_{o\sigma} = \beta_1 |o\,\sigma> + \sum_k \beta_{2k} a_{k\sigma} |2\,\sigma> + \sum_k \beta_{2k} a_{k-\sigma} |2\,e> + \sum_k \beta_{3k} b_{k-\sigma} |2\,o> \qquad (4.13b)$$

where the α 's and β's are variational parameters and the b's and a's are the conduction electron operators defined in eqs. (2.3). We can see that the first terms in eqs. (4.13) are just the unperturbed doublet basis states and the rest of the wave function comes from the coupling between the spin-half conduction electrons and doubly occupied impurity states. Let $z_{e\sigma}$ be the energy of the even state, where (cf. eq. (2.9))

$$z_{e\sigma} = \frac{<\Phi_{e\sigma}|H_1|\Phi_{e\sigma}>}{<\Phi_{e\sigma}|\Phi_{e\sigma}>} \qquad (4.14)$$

Imposing the condition

$$\delta z_{e\sigma} = 0$$

we obtain the variational equations

$$(z_{e\sigma} - E_{e\sigma})\alpha_0 = \sum_k \sqrt{2}\, V_- \alpha_{1k} + \sum_k V_- \alpha_{2k} - \sum_k V_+ \alpha_{3k} \tag{4.15a}$$

$$(z_{e\sigma} + \varepsilon_k - E_{2\sigma})\alpha_{1k} = \sqrt{2}\, V_- \alpha_0 \tag{4.15b}$$

$$(z_{e\sigma} + \varepsilon_k - E_{2e})\alpha_{2k} = V_- \alpha_0 \tag{4.15c}$$

$$(z_{e\sigma} + \varepsilon_k - E_{2o})\alpha_{3k} = - V_+ \alpha_0 \tag{4.15d}$$

The energy levels $E_{2\sigma}$, E_{2e} and E_{2o} of the doubly occupied states would split from their original value $2\varepsilon_f$ due to the RKKY interaction at high temperatures as discussed earlier. This effect has to be accounted for when one wants to calculate the low temperature properties. Therefore as before in this chapter we shall set $E_{2\sigma}$ and E_{2e} to $2\varepsilon_f - \frac{I}{2}$ and E_{2o} to $2\varepsilon_f + \frac{I}{2}$ (we shall do the same for the singlet state wave function calculation later on). This is equivalent to neglecting all high order contributions while adding an effective interaction $I(\vec{S}_1 \cdot \vec{S}_2 - \frac{1}{4})$ to the model Hamiltonian of eq. (2.2). Substituting eqs. (4.15b) (4.15c) and (4.15d) into eq. (4.15a) we get the eigenvalue equation

$$z_{e\sigma} - \varepsilon_f = \sum_k \frac{3V_-^2}{z_{e\sigma} + \varepsilon_k - 2\varepsilon_f + \frac{I}{2}} + \sum_k \frac{V_+^2}{z_{e\sigma} + \varepsilon_k - 2\varepsilon_f - \frac{I}{2}} \tag{4.16a}$$

Similarly for the state $|o\sigma>$ we have

$$z_{o\sigma} - \varepsilon_f = \sum_k \frac{3V_+^2}{z_{o\sigma} + \varepsilon_k - 2\varepsilon_f + \frac{I}{2}} + \sum_k \frac{V_-^2}{z_{o\sigma} + \varepsilon_k - 2\varepsilon_f - \frac{I}{2}} \tag{4.16b}$$

We can see that these equations are identical to eq. (4.11) obtained through the diagrammatical self-energy calculation.

The trial wave function for the singlet is constructed as

$$|\Phi_s> = \alpha_0|0> + \sum_{k\sigma} \frac{\alpha_{1k}}{\sqrt{2}} a_{k\sigma}|e\sigma> + \sum_{k\sigma} \frac{\alpha_{2k}}{\sqrt{2}} b_{k\sigma}|o\sigma>$$

$$+ \sum_{kk'} \frac{\beta_{1kk'}}{\sqrt{3}} \left(\sum_\sigma a_{k\sigma} b_{k'\sigma}|2\sigma> + \frac{1}{\sqrt{2}}(a_{k\uparrow} b_{k'\downarrow} + a_{k\downarrow} b_{k'\uparrow})|2e>\right)$$

$$+ \sum_{kk'} \frac{1}{\sqrt{3}} (\beta_{2kk'} a_{k\uparrow} a_{k'\downarrow} - \beta_{3kk'} b_{k\uparrow} b_{k'\downarrow})|2o> \tag{4.17}$$

where the first term is the unperturbed Fermi sea singlet, the second and the third terms come from the antiferromagnetic pairing of the spin-half impurity doublet and the spin-half conduction electrons and the last two terms come from the coupling between the

doubly occupied impurity states and the two conduction electron channels. The variational equations are

$$z_0\alpha_0 = \sum_{k\sigma} V_+\alpha_{1k} + \sum_{k\sigma} V_-\alpha_{2k} \tag{4.18a}$$

$$(z_0 + \varepsilon_k - \varepsilon_f)\alpha_{1k} = -\sqrt{3}\sum_{k'} V_-\beta_{1kk'} + \frac{1}{\sqrt{3}}\sum_{k'} V_+\beta_{2kk'} + 2\alpha_0 V_+ \tag{4.18b}$$

$$(z_0 + \varepsilon_k - \varepsilon_f)\alpha_{2k} = -\sqrt{3}\sum_{k'} V_+\beta_{1k'k} + \frac{1}{\sqrt{3}}\sum_{k'} V_-\beta_{3k'k} + 2\alpha_0 V_- \tag{4.18c}$$

$$(z_0 + \varepsilon_k + \varepsilon_{k'} - 2\varepsilon_f + \frac{I}{2})\beta_{1kk'} = -\sqrt{3}\,(V_-\alpha_{1k} + V_+\alpha_{2k'}) \tag{4.18d}$$

$$(z_0 + \varepsilon_k + \varepsilon_{k'} - 2\varepsilon_f - \frac{I}{2})\beta_{2kk'} = -\sqrt{3}\,V_+(\alpha_{1k} + \alpha_{1k'}) \tag{4.18e}$$

$$(z_0 + \varepsilon_f + \varepsilon_{k'} - 2\varepsilon_f - \frac{I}{2})\beta_{3kk'} = -\sqrt{3}\,V_-(\alpha_{2k} + \alpha_{2k'}) \tag{4.18f}$$

Define

$$\alpha_{1k} = \frac{\alpha_{1k}}{2\alpha_0 V_+} \qquad \alpha_{2k} = \frac{\alpha_{2k}}{2\alpha_0 V_-}$$

and

$$\beta_{ikk'} = \frac{\beta_{ikk'}}{2\alpha_0}$$

where i runs from 1 to 3, and substitute eq. (4.18d) (4.18e) and (4.18f) into eq. (4.18a) (4.18b) and (4.18c); we get

$$z_0 = 2\sum_{k\sigma} V_+^2 \alpha_{1k} + 2\sum_{k\sigma} V_-^2 \alpha_{2k} \tag{4.19a}$$

$$\alpha_{1k} = \frac{1}{z_0 + \varepsilon_k - \varepsilon_f}\left(1 + 3V_-^2 \sum_{k'} \frac{\alpha_{1k} + \alpha_{2k'}}{z_0 + \varepsilon_k + \varepsilon_{k'} - 2\varepsilon_f + \frac{I}{2}}\right.$$

$$\left. + V_+^2 \sum_{k} \frac{\alpha_{1k} + \alpha_{1k'}}{z_0 + \varepsilon_k + \varepsilon_{k'} - 2\varepsilon_f - \frac{I}{2}}\right) \tag{4.19b}$$

$$\alpha_{2k} = \frac{1}{z_0 + \varepsilon_k - \varepsilon_f}\left(1 + 3V_+^2 \sum_{k'} \frac{\alpha_{1k'} + \alpha_{2k}}{z_0 + \varepsilon_k + \varepsilon_{k'} - 2\varepsilon_f + \frac{I}{2}}\right.$$

$$\left. + V_-^2 \sum_{k'} \frac{\alpha_{2k} + \alpha_{2k'}}{z_0 + \varepsilon_k + \varepsilon_{k'} - 2\varepsilon_f - \frac{I}{2}}\right) \tag{4.19c}$$

Here the α_{1k} and α_{2k} are exactly the same as the A and B in eqs. (4.10). We can see this by moving the α_{1k}, α_{2k} terms on the right hand sides of eq. (4.19b) and (4.19c) to the left

hand sides. Then those terms are seen to be just the lowest order self-energies of eq. (4.11) for the singly occupied states. So once again the two methods give us the same results. The calculation in this section confirms that the f_0 state has lower energy than the f_1 state. The difference is of order $T_{K\pm}$. Thus we can confidently conclude that the ground state is indeed a singlet.

Calculations on the two-impurity Anderson model have also been done by other groups (18,23,29) using different techniques. Jones and Varma (23) have used the numerical renormalization group method to study the behaviour of the two-impurity Kondo system. By examining the "flow" of the model Hamiltonian they derive an effective Hamiltonian at low temperature in different regimes. In the limit $|I| > T_k$ their results are essentially the same as that of scaling and ours. In contrast to general belief however, they found that the system still behaves as a correlated Kondo system even in the range $|I| < T_k$. This means that the ground state would be quite different from that of the single impurity even if the initial intersite interaction is small at high temperature, because it will become bigger and eventually diverges at very low temperatures. In our calculation we find that the originally existing divergences for the intersite interactions disappear after taking renormalization from Kondo effect into account as discussed in chapter 3 and in ref. (24). The residual interaction between the impurities is still small so that the correlations are negligible. Hirsch and Fye (29) have calculated the magnetic susceptibility and the spin-spin correlation function by using the Monte Carlo method. They show that the two impurities are not likely to form a spin triplet in the limit $I \leq T_k$, which is in disagreement with Varma's results. This difference is yet to be understood.

Diagrammatical techniques have also been utilized by other people (14,18) in approaching the two-impurity Anderson model. Coleman (18,26) solved the problem first at the mean field level and then considered the fluctuations by using the 1/N expansion method first developed for the single impurity model. He proceeded to calculate the dynamic and static magnetic susceptibility at the 1/N level. He also derived the Fermi liquid propertities of the system which were first discussed by Nozieres (25). Since the RKKY interaction for the impurities is of order of $1/N^2$, its role is not manifested in Coleman's calculation. More discussions on the two-impurity model can be found in two recently published review articles (27, 28) and references therein.

Chapter 5: Conclusion

We have successfully applied the perturbative diagrammatic technique to the two-impurity Anderson model in the Kondo regime. Naturally the complexity of the Hamiltonian makes the diagrammatic calculations more complicated than in the single impurity case. The emergence of the intersite interactions, mainly the RKKY interaction gives one new physics and makes the system more interesting. The system behave differently depending on the strength and the sign of the interaction between the impurities. If the magnitude of the RKKY interaction I is smaller than the Kondo temperature T_k of the single impurity system it has little effect on the properties of the system since the impurities will be screened by the conduction electrons first and the intersite interaction only gives a negligible contribution. If I is negative and the magnitude is large, i.e., if the interaction is antiferromagnetic, then the two impurities will pair up into a singlet and Kondo screening by conduction electrons will not happen. The reason for this is that the magnetic interactions between the impurities and the conduction electrons which are responsible for the Kondo screening are absent now because the impurities themselves have already formed a singlet and have no marnetic moment.

The most interesting case is when the RKKY interaction is strong and positive. In this situation the competition between the ferromagnetic coupling of impurities and the antiferromagnetic screening of conduction electrons is in favor of ferromagnetic pairing at high temperatures, so the two impurities will form a spin-one triplet first. As temperature lowers the impurities will be screened gradually, first by the odd-channel electrons to form an effective spin one-half particle with complicated internal structure and then by the even channel electrons to become a spin singlet. This is the so-called " two-stage " Kondo effect. There are two energy scales besides the RKKY interaction associated with the two-stage Kondo screening. The first energy scale can be obtained from the high temperature perturbative expansion series for magnetic susceptibility as discussed in chapter 3. It is just the temperature at which the susceptibility diverges. The second energy scale and the ground state energy are obtained through the zero temperature selfenergy calculations. A set of integral equations is found for the ground state energy by including the 1/N leading order diagrams of the unoccupied state and the renormalization due to the first stage Kondo screening. Unlike the single impurity case the crossed diagrams are important and result in two coupled integral equations. After solving the equations numerically we found that the unoccupied state has lower energy than the singly and doubly occupied states at zero temperature, which means the ground state is a singlet, i.e. the spins of the impurities are totally screened by the conduction electrons. We have also constructed trial wave functions for each of the states and calculated the corresponding energies. This variational calculation confirms to the diagrammatic results and shows that the ground state is indeed a singlet.

Further applications of the diagrammatic methods to the two-impurity Anderson model for the calculations of various physical quantitiess like magnetic susceptibility, specific heat and resistivity at low temperatures would be very interesting and the calculations

should be straightforward. The intersite contributions to the properties of heavy fermion superconductor systems can then be compared with the experimental results. The extension to arbitary spin system should be practical although the calculations are more complicated due to the multiplicity of the total-spin magnetic states resulting from the coupling between the impurities. Instead splitting between the triplet and the singlet due to the RKKY interaction in the spin-half case one has to examine the energy differences between all the states due to the RKKY interaction and consider the screening from there. One of the drawbacks of this diagrammatic method is that it is difficult to extend to the lattice case because of its complexity.

References:

(1) "Valence Fluctuation in Solids " ed. by L. M. Falicov, W. Hanke and M. B. Maple (North Holland, Amsterdam, 1981)

(2) Proceedings of The International Conference on Valence Instabilities " ed. by P. Wachter (North Holland, Amsterdam, 1982)

(3) G. P. Stewart, Rev. Mod. Phys. **56** , 755 (1984) and references therein.

(4) P. W. Anderson, Phys. Rev. **126** , 41 (1961); B. Coqblin and J. R. Shrieffer, Phys. Rev. **185** , 847 (1969)

(5) J. R. Shrieffer and P. A. Wolff, Phy. Rev. **149** , 491 (1966)

(6) J. Kondo, in "Solid State Physics" Vol. 23, eds. F. Seitz, D. Turnbull, and H. Ehrenreich (Academic Press, New York, 1969) p. 183

(7) K.G. Wilson, Rev. Mod. Phys. **47** , 773 (1975)

(8) N. Andrei, K. Furuga and J. H. Lowenstein, Rev. Mod. Phys. **55** , 331 (1983)

(9) F. Steglich, J. Aarts, C. D. Bredl, W. Lieke, D. Meshede, W. Franz, and H. Schafer, Phys. Rev. Lett. **43** , 1892 (1979)

(10) G. R. Stewart, Z. Fisk, J. O. Willis and J. L. Smith, Phys. Rev. Lett., **52** , 697 (1984)

(11) H. R. Ott, H. Rudigier, Z. Fisk and J. L. Smith, Phys. Rev. Lett., **50** , 1595 (1983)

(12) H. Keiter and J.C. Kimball, Int. J. Magn. **1** , 233 (1971); H. Keiter and N. Grewe, Phys. Rev. **B24** , 4420 (1981)

(13) F. C. Zhang and T.K. Lee, Phys. Rev. **B28** , 33 (1983). F. C. Zhang and T. K. Lee, Phys. Rev. **B30** , 1556 (1984).

(14) J.W. Rasul and H.C. Hewson, Solid State Comm. **52** , 217 (1984)

(15) P. Colman, Phys. Rev. **B28** , 5255 (1983)

(16) T.V. Ramakrishnan p. 13 Ref. (1); P.W. Anderson p. 451 Ref. (1)

(17) C. Jayaprakash, H.R. Krishnan-murthy and J.W. Wilkins, Phys. Rev. Lett. **47** , 737 (1981).

(18) P. Colman, Phys. Rev., **B29** , 3035 (1984) P. Coleman, J Magn. Magn. mat. **52** , 223 (1985b)

(19) E. Abraham and C.M. Varma, The Theory of Fluctuating Valance State, ed. by T. Kaysuya (S pringer-Verlag, New York, 1985)

(20) N. Read, K. Dharamvir, J. W. Rasul and D. M. Newns, J. Phys. C, **19** , 1597 (1986)

(21) P.W. Anderson, J. Phys. **C3** , 2436 (1970)

(22) C.M. Varma and Y. Yafet, Phys. Rev. **B13** , 295 (1975)

(23)B. A. Jones and C.M. Varma, Phys. Rev. Lett. **58** , 843 (1987). B. Jones and C. M. Varma, J. Magn. Magn. Mat. **63&64** , 251 (1987).

(24) C. Zhou and T. K. Lee, J. Magn. Magn. Mat. **63&64** , 248 (1987).

(25) P. Nozieres, J. Low Temp. Phys. **17** , 31 (1974).

(26) P. Coleman, in " Theory of Heavy Fermions and Valence Fluctuations " eds. T. Kasuga and T. Saso (Springer Verlag, Berlin, 1985c) p. 163.

(27) P. Fulde, J. Keller and G. Zwicknagl, Preprint.

(28) P. A. Lee, T. M. Rice., J. w. Serene, L. J. Sham and J. W. Wilkins, Comments on Condensed Matter Physics, **12** , 99 (1986)

(29) J. E. Hirsch and R. M. Fye, Phys. Rev. Lett., **56** , 2521 (1986)

Appendix

A. A sample of the integral evaluation

$$I_1 = \sum_k \frac{(1-f_k)\sin kR}{(\epsilon_k-\epsilon_F)kR} = \int_{\epsilon_F+T}^{\epsilon_F+D} \rho d\epsilon_k \frac{\sin kR}{(\epsilon_k-\epsilon_F)kR}$$

$$= \int_{k_F+\frac{Tm}{k_F}}^{k_F+\frac{Dm}{k_F}} \rho dk \frac{k\sin kR}{m(\epsilon_k-\epsilon_F)kR} = 2\rho\int dk \frac{k\sin kR}{(k^2-k_F^2)kR}$$

$$= 2\rho \int_{\frac{Tm}{k_F}}^{\frac{Dm}{k_F}} dk' \frac{(k'+k_F)(\sin k'R\cos k_FR + \cos k'R\sin k_FR)}{k'(k'+2k_F)(k'+k_F)R}$$

where

$$\epsilon_k = \frac{k^2}{2m} \qquad \epsilon_F = D = \frac{k_F^2}{2m} \qquad k' = k - k_F$$

Expanding around $k' = 0$ and keeping the lowest and next lowest order terms only

$$I_1 = \frac{\rho}{k_F}\int_{\frac{Tm}{k_F}}^{\frac{Dm}{k_F}} dk' \left[\frac{\cos k_FR\sin k'R}{k'R} + \frac{\sin k_FR\cos k'R}{k'R}\right]$$

$$= \frac{\rho}{k_FR}\left[\frac{\pi}{2}\cos k_FR + \sin k_FR\ln D/T\right]$$

Similarly:

$$I_2 = \sum_k \frac{-f_k\sin kR}{(\epsilon_k-\epsilon_F)kR} = \frac{\rho}{k_FR}\left[-\frac{\pi}{2}\cos k_FR + \sin k_FR\ln D/T\right]$$

B. Diagrams Contributing to eq.(3.8)

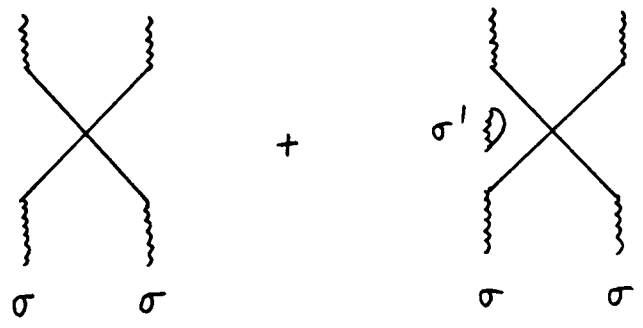

(1) (2)

The diagrammatical rules used here are given by Grewer and Keiter in reference (12)

$$Z^{(1)} = -\sum_{n,\sigma} n_\sigma^2 \beta^{-2} g^2(w_n) \left[\frac{-\beta}{2\pi i} \int dz \frac{e^{-\beta z}}{z(z+\epsilon_\sigma - iw_n)} \right]^2$$

$$= -\sum_{n,\sigma} n_\sigma^2 g^2(w_n) \frac{1}{(\epsilon_\sigma - iw_n)^2} = \sum_\sigma n_\sigma^2 \frac{I}{2T}$$

where

$$g(w_n) = \sum_k \frac{V^2 e^{i\vec{k}\cdot\vec{R}}}{iw_n - \epsilon_k} = \sum_k \frac{i \sin kR \; V^2}{kR \; (iw_n - \epsilon_k)}$$

$$I = -2T \sum_n \frac{g^2(w_n)}{(\epsilon_\sigma - iw_n)^2} = \frac{2V^4}{\epsilon_f^2} \sum_{kk'} \frac{2 f_k \sin\alpha_1 \sin\alpha_2}{(\epsilon_1 - \epsilon_2)\alpha_1 \alpha_2}$$

Here we have used the condition $|\varepsilon_f| >> i\omega_n$ for small n and $\alpha_i = k_i R$

$$\chi^{(1)} = \frac{1}{\beta} \frac{\partial^2 Z^{(1)}}{\partial H^2} = \frac{1}{\beta} \sum_\sigma \frac{I}{2T} \frac{\partial^2 n_\sigma^2}{\partial H^2} = \frac{I}{T^2} \sum_\sigma n_\sigma^2 \sigma^2$$

$$= \frac{I}{8T^2}$$

where

$$n_\sigma = \frac{e^{-\beta\epsilon_\sigma}}{1+\sum_{\sigma'} e^{-\beta\epsilon_{\sigma'}}} \approx \frac{1}{2} \qquad \epsilon_\sigma = \epsilon_f - \sigma H \qquad \sigma^2 = \frac{1}{4}$$

$$Z^{(2)} = -\sum_{\sigma\sigma'} n_\sigma^2 \beta^{-2} \sum_n g^2(i\omega_n)\left(\frac{-\beta}{2\pi i}\right)\int d\zeta_2 \frac{e^{-\beta\zeta_2}}{\zeta_2(\zeta_2+\epsilon_\sigma-i\omega_n)}$$

$$\times \frac{-\beta}{2\pi i}\int d\zeta_1 \frac{e^{-\beta\zeta_1}}{\zeta_1}\sum_k \frac{V^2 f_k}{(\zeta_1+\epsilon_\sigma-i\omega_n)^2(\zeta_1+\epsilon_\sigma-i\omega_n+\epsilon_k-\epsilon_{\sigma'})}$$

$$= -\sum_{\sigma\sigma'} n_\sigma \sum_n g^2(i\omega_n)\frac{1}{\epsilon_f^3}\left[\sum_k\left(\frac{V^2 f_k n_\sigma}{(\epsilon_\sigma-\epsilon_{\sigma'}+\epsilon_k-i\omega_n)} + \frac{V^2(1-f_k)n_{\sigma'}}{(\epsilon_\sigma-\epsilon_{\sigma'}+\epsilon_k-i\omega_n)}\right)\right]$$

$$= -\beta\sum_{\sigma\sigma'} n_\sigma \sum_{k_1k_2}\sum_k \frac{2f_1 V^6 f_k \sin\alpha_1 \sin\alpha_2}{(\epsilon_1-\epsilon_2)\epsilon_f^3(\epsilon_k-\epsilon_1+\epsilon_\sigma-\epsilon_{\sigma'})}\left[f_k n_\sigma + n_{\sigma'}(1-f_k)\right]$$

The leading order contribution to the magnetic susceptibility comes from taking the first order derivative with respect to $n_\sigma (n_{\sigma'})$ and $\varepsilon_\sigma (\varepsilon_{\sigma'})$ once each so the contribution from the second term disappears.

$$\chi^{(2)} = \frac{1}{\beta}\frac{\partial^2 Z^{(2)}}{\partial H^2} = -\sum_{\sigma\sigma'} 2\frac{\partial n_\sigma^2}{\partial H}\sum_{\substack{k_1k_2\\k}} \frac{2f_1 f_k \sin\alpha_1\sin\alpha_2 V^4}{\epsilon_f^3(\epsilon_1-\epsilon_2)\alpha_1\alpha_2}\frac{\partial}{\partial H}\frac{1}{\epsilon_k-\epsilon_1+\epsilon_\sigma-\epsilon_{\sigma'}}$$

$$= -\sum_{\sigma\sigma'} 4(-\beta)n_\sigma^2\left(\frac{\partial\epsilon_\sigma}{\partial H}\right)^2\sum_{\substack{k_1k_2\\k}} \frac{2f_1 f_k \sin\alpha_1\sin\alpha_2 V^4}{\epsilon_f^3(\epsilon_1-\epsilon_2)\alpha_1\alpha_2}\frac{\partial}{\partial\epsilon_1}\frac{-1}{\epsilon_k-\epsilon_1+\epsilon_\sigma-\epsilon_{\sigma'}}$$

Integrating by parts in the integral respect to ε_k and using

$$\frac{\partial f_k}{\partial\epsilon_k} = \frac{\partial}{\partial\epsilon_k}\frac{1}{1+e^{\beta\epsilon_k}} = -\rho\,\delta(\epsilon_k)$$

we have

$$\chi^{(2)} = \sum_{\sigma\sigma'} -4\beta n_\sigma^2 \sigma^2 \sum_{k k_2} \frac{2\rho V^6 f_k \sin\alpha_F \sin\alpha_2}{\alpha_F \alpha_2 (-\epsilon_2)\epsilon_k \epsilon_f^3}$$

$$= \frac{J^3 \pi \sin 2\alpha_F}{8\alpha_F^2} \ln T/D$$

C. Diagrams contribuiting to eq. (3.10)

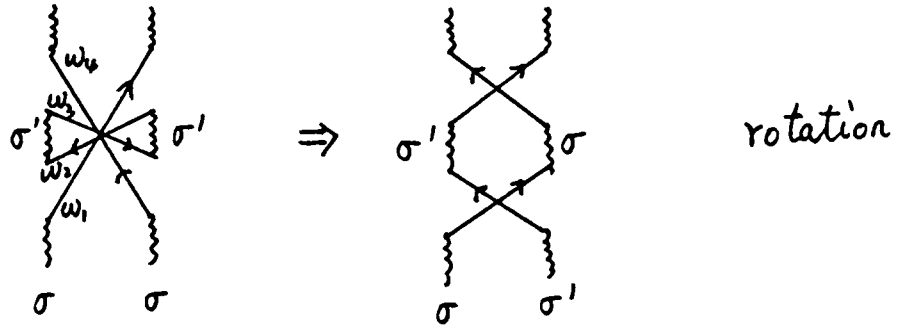

$$Z = \frac{1}{2}\sum_{\sigma\sigma'} n_\sigma^2 \beta^{-4} \sum_{n_i} \prod_i g(i\omega_i)\, \delta(\omega_1 - \omega_2 + \omega_3 - \omega_4)$$

$$\left[\frac{-\beta}{2\pi i}\int d\zeta \frac{e^{-\beta\zeta}}{\zeta(\zeta+\epsilon_\sigma - i\omega_1)(\zeta+\epsilon_\sigma - i\omega_1 + i\omega_2 - i\omega_3)(\zeta+\epsilon_\sigma - \epsilon_{\sigma'} - i\omega_1 + i\omega_2)}\right]^2$$

$$= \frac{1}{2}\sum_{\sigma\sigma'} (n_\sigma - n_{\sigma'})^2 \sum_n \frac{\prod g(i\omega_1)\, \delta(\omega_1 - \omega_2 + \omega_3 - \omega_4)}{\epsilon_f^4 \beta^2 (i\omega_1 - i\omega_2 - \epsilon_\sigma + \epsilon_{\sigma'})^2}$$

The factor 1/2 come from the rotation symmetry. It is a good approximation to neglect $(\omega_1 - \omega_2)$ in the delta function since it is very small (of the order $(\varepsilon_1 - \varepsilon_2)$.)

$$Z = \frac{1}{2}\sum_{\sigma\sigma'}(n_\sigma - n_{\sigma'})^2 \sum_n \frac{g^2(\omega_n)}{\epsilon_f^4} \sum_{k_1 k_2} \frac{V^4 f_1 f_2 \sin\alpha_1 \sin\alpha_2}{\alpha_1\alpha_2(-\epsilon_1+\epsilon_2+\epsilon_\sigma-\epsilon_{\sigma'})^2}$$

$$\chi = \frac{1}{4}\sum_{\sigma\sigma'}\left(2T\sum_n \frac{g^2(\omega_n)}{\epsilon_f^2}\right)\sum_{k_1 k_2} \frac{V^4 f_1 f_2 \sin\alpha_1 \sin\alpha_2}{\epsilon_f^2 \alpha_1\alpha_2(\epsilon_2-\epsilon_1)^2}\frac{\partial^2}{\partial H^2}(n_\sigma - n_{\sigma'})^2$$

$$= \frac{-I}{4}\sum_{\sigma\sigma'} n_\sigma^2\sigma^2 \frac{8V^4}{\epsilon_f^2}\sum_{k_1 k_2}\frac{\beta^2 f_1 f_2 \sin\alpha_1 \sin\alpha_2}{\alpha_1\alpha_2}\frac{\partial}{\partial\epsilon_1}\frac{1}{\epsilon_2-\epsilon_1}$$

$$= \frac{-I\rho V^4\beta^2}{2\epsilon_f^2}\sum_{k_2}\frac{f_2 \sin\alpha_2 \sin\alpha_F}{\alpha_2\alpha_F\epsilon_2} = \frac{I\beta^2(\rho J)^2\sin^2\alpha_F}{8\alpha_F^2}\ln T/D$$

D. Diagrams contributiong to eq. (3.11)

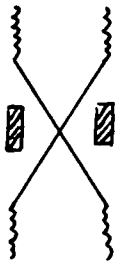

$$\sigma \Rightarrow \text{(loop)} = S^0(z) = \sum_{\sigma k}\frac{f_k V^2}{z+\epsilon_k-\epsilon_\sigma}$$

$$Z = -\sum_\sigma n_\sigma^2 \sum_n \beta^{-2} g^2(\omega_n)\left(\frac{-\beta}{2\pi i}\int dz \frac{e^{-\beta z}}{z(z+\epsilon_\sigma - i\omega_n - S^0)}\right)^2$$

$$= -\sum_\sigma n_\sigma^2 \sum_n g^2(\omega_n)\frac{e^{-2\beta(E_0-\epsilon_\sigma)}}{(1-S^{0\prime})^2(E_0-\epsilon_\sigma+i\omega_n)^2}$$

where E_0 is the solution of the equation $E_0 - S^0(E_0) = 0$ Since we are in the regime T << T_k we can neglect the poles at $i\omega_n + E_0 - \varepsilon_\sigma$ because $|E_0 - \varepsilon_\sigma| \cong T_k >> T$.

$$Z = \frac{1}{T} \sum_{\sigma} n_0^2 e^{-2\beta E_0} \sum_{k_1 k_2} \frac{2V^4 f_1 \sin\alpha_1 \sin\alpha_2}{\alpha_1 \alpha_2 (\epsilon_1 - \epsilon_2)(1-S^{0\prime})^2 (E_0 - \epsilon_\sigma + \epsilon_1)^2}$$

$$= \frac{-1}{T} \sum_{\sigma} n_0^2 e^{-2\beta E_0} \sum_{k_1} \frac{2\pi f_1 \rho V^4 \sin\alpha_1 \cos\alpha_1}{\alpha_1^2 (E_0 - \epsilon_\sigma + \epsilon_1)^2 (1-S^{0\prime})^2}$$

The partion function Z has to be divided by $Z_0^2 = (n_0 e^{-\beta E_0})^2$ which is the single site partition function renormalization due to S_0. Using

$$S^{0\prime} = \frac{d}{dz} S^0(z)\Big|_{z=E_0} = -\frac{2\rho V^2}{T_K} \quad , \quad \left(\frac{\partial \epsilon_\sigma}{\partial H}\right)^2 = \sigma^2 \quad ,$$

$$\frac{\partial^2 E_0}{\partial H^2} = -\frac{1}{T_K}\left(\frac{\partial \epsilon_\sigma}{\partial H}\right)^2 \qquad \text{and} \qquad E_0 - \epsilon_\sigma = -T_K$$

we have

$$\chi = \frac{1}{\beta} \frac{\partial^2}{\partial H^2} Z/Z_0^2 = -\pi \sum_{\sigma} \frac{\partial^2}{\partial H^2} \sum_{k_1} \frac{2\rho V^4 f_1 \sin\alpha_1 \cos\alpha_1}{\alpha_1^2 (1-S^{0\prime})^2} \frac{\partial}{\partial \epsilon_1} \frac{-1}{E_0 - \epsilon_\sigma + \epsilon_1}$$

$$= \pi \sum_{\sigma k} \frac{\rho^2 V^4 \sin 2\alpha_F}{\alpha_F^2 (1-S^{0\prime})^2} \frac{\partial^2}{\partial H^2} \frac{1}{E_0 - \epsilon_\sigma}$$

$$= \pi \sum_{\sigma} \frac{\rho^2 V^4 \sin 2\alpha_F}{\alpha_F^2 (1-S^{0\prime})^2} \left(\frac{-\frac{\partial^2 E_0}{\partial H^2}}{(E_0 - \epsilon_\sigma)^2} + \frac{2\left(\frac{\partial \epsilon_\sigma}{\partial H}\right)^2}{(E_0 - \epsilon_\sigma)^3} \right)$$

$$= -\frac{\pi \sin 2\alpha_F}{8 \alpha_F^2 T_K} \qquad (3.11)$$

E. Diagrams contributing to eq. (3.12)

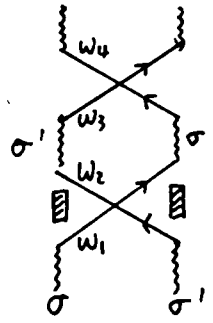

$$Z = \sum_{\sigma\sigma'} n_\sigma n_{\sigma'} \beta^{-4} \sum_{n_i} \prod_i g(i\omega_i)\, \delta(\omega_1-\omega_2+\omega_3-\omega_4) \times$$

$$\left(\frac{-\beta}{2\pi i}\right)^2 \int d\zeta_1 \frac{e^{-\beta\zeta_1}}{\zeta_1(\zeta_1+\epsilon_\sigma-i\omega_1-S^0)(\zeta_1+\epsilon_\sigma-i\omega_1+i\omega_2-\epsilon_{\sigma'})(\zeta_1+\epsilon_\sigma-i\omega_1+i\omega_2-i\omega_3)}$$

$$\times \int d\zeta_2 \frac{e^{-\beta\zeta_2}}{\zeta_2(\zeta_2+\epsilon_{\sigma'}-i\omega_2-S^0)(\zeta_2+\epsilon_{\sigma'}-i\omega_2+i\omega_1-\epsilon_\sigma)(\zeta_1+\epsilon_{\sigma'}-i\omega_2+i\omega_1-i\omega_4)}$$

$$= \sum_{\sigma\sigma'} n_0^2 e^{-2\beta E_0} \beta^{-2} \sum_{n_i} \prod_i g(i\omega_i)\delta(\omega_1-\omega_2+\omega_3-\omega_4) \frac{1}{(1-S^{0\prime})^2 (E_0+i\omega_2-i\omega_3)^2}$$

$$\times \frac{1}{(E_0-\epsilon_\sigma+i\omega_1)^2 (E_0-\epsilon_{\sigma'}+i\omega_2)^2}$$

$$= \sum_{\sigma\sigma'} n_0^2 e^{-2\beta E_0} \sum_n \frac{g^2(\omega_n)}{E_0^2} \sum_{k_1,k_2} \frac{V^4 f_1 f_2 \sin\alpha_1 \sin\alpha_2}{\alpha_1\alpha_2 (1-S^{0\prime})^2 (E_0-\epsilon_\sigma+\epsilon_1)^2 (E_0-\epsilon_{\sigma'}+\epsilon_2)^2}$$

$$= -\frac{\beta}{2} \sum_{\sigma\sigma'} n_0^2 e^{-2\beta E_0} I \frac{\sin^2\alpha_F \; T_K^2}{4\alpha_F^2 (E_0-\epsilon_\sigma)(E_0-\epsilon_{\sigma'})}$$

The approximation made here in frequency summation is the same as in appendix C.

$$\chi = \frac{1}{\beta}\frac{\partial^2}{\partial H^2}\frac{Z}{Z_0}^2 = \sum_\sigma \frac{I \sin^2\alpha\, T_K^2}{4\alpha^2(E_0-E_\sigma)} \sum_{\sigma'} \frac{\partial^2}{\partial H^2}\frac{1}{E_0-\epsilon_{\sigma'}}$$

$$= \frac{I \sin^2\alpha\, T_K^2}{2\alpha^2(E_0-\epsilon_\sigma)} \sum_{\sigma'} \left(\frac{-\frac{\partial^2 E_0}{\partial H^2}}{(E_0-\epsilon_\sigma)^2} + \frac{2\left(\frac{\partial \epsilon_{\sigma'}}{\partial H}\right)^2}{(E_0-\epsilon_\sigma)^3} \right)$$

$$= \frac{I \sin^2\alpha\, T_K^2}{4\alpha^2(E_0-\epsilon_\sigma)^4} = \frac{I \sin^2\alpha}{4\alpha^2 T_K^2}$$

F. Diagrams contributing to eq. (3.16)

The diagrammatic rules used here are derived from the symmetrized two impurity Kondo Hamiltonian eq. (3.13). The rules are essentially the same as those described in section 2.2. The only difference is that all singly occupied stats are now eliminated, i.e. their contributions to the energy denominators are taken to be constants ε_f which combine with $2V^2$ and become coupling constant J. It is illustrated diagrammatically as

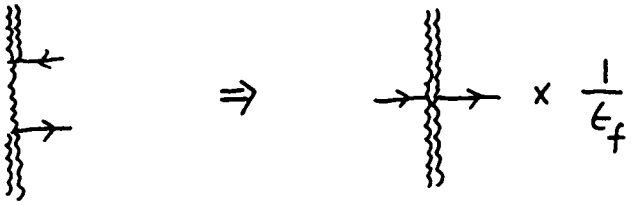

Taking into account the renormalizatoins due to the RKKY interaction the energies of the four doubly occupied states are $E_{2\sigma} = E_{2\sigma} = 2\varepsilon_f - \frac{I}{2}$ and $E_{2o} = 2\varepsilon_f + \frac{I}{2}$. For the sake of simplicity we will represent state 2↑ as 1, state2e as 2, state 2↓ as 3 and state 2o as 0. Here are some rules regarding the factors and the signs to a diagram we want to state again. a) Each potential scattering vertex (ρ) gives a factor 1 while each spin flip scattering ($S^{\pm}$) gives a factor -1. b) States 2σ (1 and 3) give a factor 1 while states 2e and

2o (2 and 0) gives a factor 1/2. c) Each crossing gives a factor -1 and each $\rho_{ab\uparrow}$ gives a factor -1. (All diagrams obtained through the exchage a = b and 1 = 3 from diagrams drawn explicitely below are included in the calculation.)

The third order diagrams

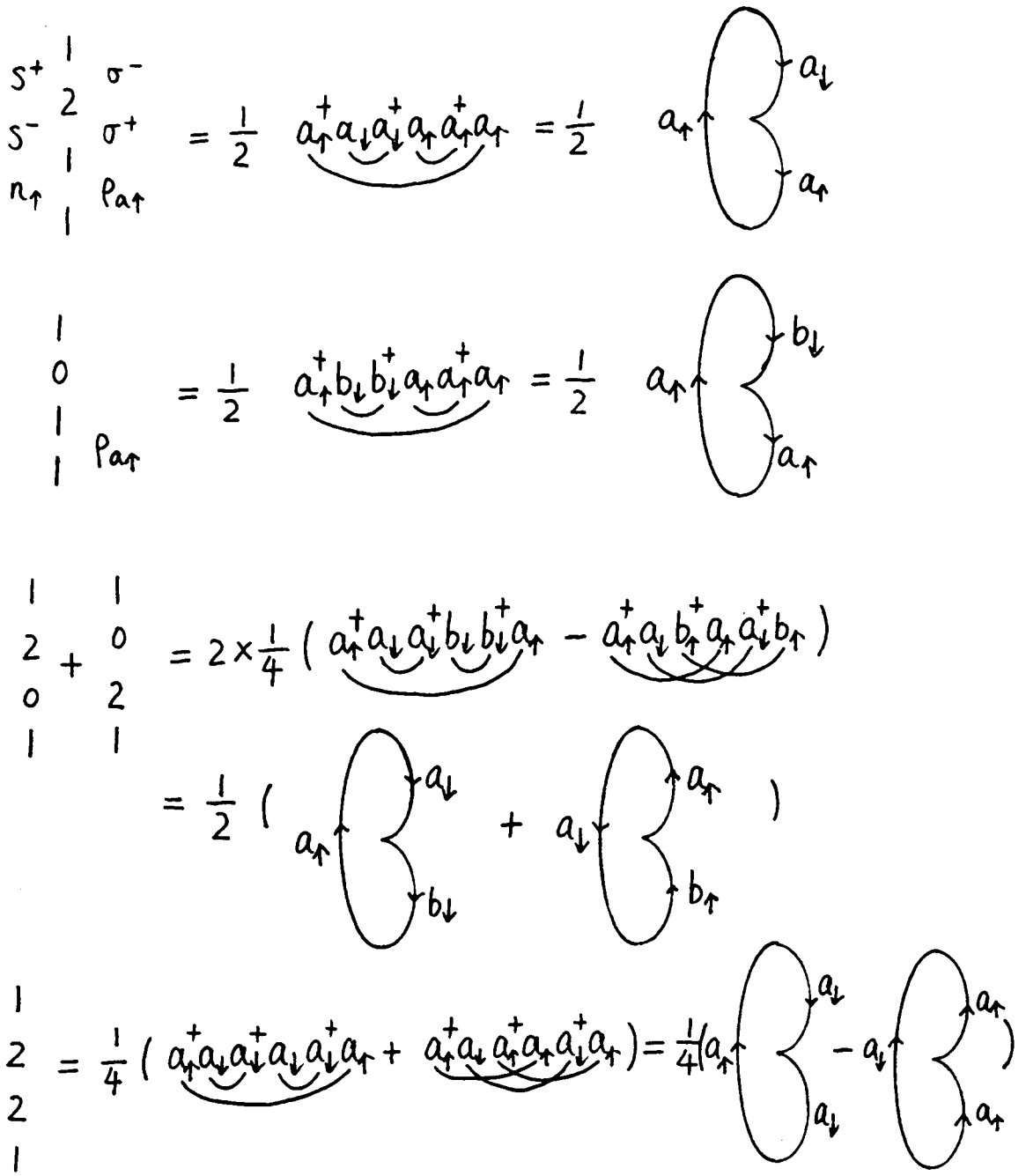

$$
\begin{matrix} 1 \\ 0 \\ 0 \\ 1 \end{matrix}
= \frac{1}{4}\left(b_\uparrow^+ a_\downarrow a_\downarrow^+ a_\downarrow a_\downarrow^+ b_\uparrow + a_\uparrow^+ b_\downarrow a_\uparrow^+ a_\uparrow b_\downarrow^+ a_\uparrow \right) = \frac{1}{4}\left(b_\downarrow \overset{a_\downarrow}{\overset{a_\downarrow}{\frown}} + b_\downarrow \overset{a_\uparrow}{\overset{a_\uparrow}{\frown}} \right)
$$

$$
Z = \frac{1}{2}\sum_\sigma n_\sigma^2 e^{\beta I/2}\left(\frac{-\beta}{2\pi i}\right)\int d\zeta\, \frac{e^{-\beta\zeta}}{\zeta}\left\{ \left(J_+^3 + J_-^3\right)\left[\frac{(1-f_1)f_2 f_3}{(\zeta+\epsilon_2-\epsilon_1)(\zeta+\epsilon_3-\epsilon_1-2\sigma H)} \right.\right.
$$

$$
+ \frac{1}{2}\frac{(1-f_1)f_2 f_3}{(\zeta+\epsilon_2-\epsilon_1-2\sigma H)(\zeta+\epsilon_3-\epsilon_1-2\sigma H)} - \frac{1}{2}\frac{f_1(1-f_2)(1-f_3)}{(\zeta+\epsilon_1-\epsilon_2-2\sigma H)(\zeta+\epsilon_1-\epsilon_3-2\sigma H)}\Big] + \left(J_+^2 J_- + J_-^2 J_+\right)
$$

$$
\left[\frac{(1-f_1)f_2 f_3}{(\zeta+\epsilon_2-\epsilon_1)(\zeta+\epsilon_3-\epsilon_1-2\sigma H-I)} + \frac{(1-f_1)f_2 f_3}{(\zeta+\epsilon_2-\epsilon_1-2\sigma H)(\zeta+\epsilon_3-\epsilon_1-2\sigma H-I)} + \frac{f_1(1-f_2)(1-f_3)}{(\zeta+\epsilon_1-\epsilon_2-2\sigma H)(\zeta+\epsilon_1-\epsilon_3-2\sigma H-I)} \right.
$$

$$
\left. + \frac{\frac{1}{2}(1-f_1)f_2 f_3}{(-I+\zeta+\epsilon_2-\epsilon_1-2\sigma H)(\zeta+\epsilon_3-\epsilon_1-2\sigma H-I)} - \frac{1}{2}\frac{f_1(1-f_2)(1-f_3)}{(\zeta+\epsilon_2-\epsilon_1-2\sigma H-I)(\zeta+\epsilon_3-\epsilon_1-2\sigma H-I)} \right]
$$

$$
= \frac{-\beta}{2}\sum_\sigma n_\sigma^2 e^{\beta I/2}\left\{ \left(J_+^3 + J_-^3\right)\frac{2(1-f_1)f_2 f_3}{(\epsilon_2-\epsilon_1)(\epsilon_3-\epsilon_1-2\sigma H)} + \left(J_+^2 J_- + J_-^2 J_+\right)\times \right.
$$

$$
\left. \left[\frac{2(1-f_1)f_2 f_3}{(\epsilon_2-\epsilon_1)(\epsilon_3-\epsilon_1-2\sigma H-I)} + \frac{2(1-f_1)f_2 f_3}{(\epsilon_2-\epsilon_1-2\sigma H)(\epsilon_3-\epsilon_1-2\sigma H-I)} \right] \right\}
$$

Here the second term and the third term in the first braket are canceled which is apparent after making the exchage $\varepsilon_i \rightarrow -\varepsilon_i$. Similarly, we have combined the second and the third term and canceled the fourth and the fifth term in the second braket. The leading order contribution to the magnetic susceptibility comes from taking first order derivative with respect to n_σ^2 and $-2\sigma H$ in the energy denominators once each as we did before.

$$Z_0 = \frac{1}{\sum_i n_i e^{-\beta\epsilon_i}} = \frac{1}{3n_\sigma^2 e^{\beta I/2} + n_\sigma^2 e^{-\beta I/2}} \cong \frac{1}{3n_\sigma^2 e^{\beta I/2}}$$

$$\chi = \frac{1}{\beta}\frac{\partial^2}{\partial H^2} Z/Z_0 = \frac{4\beta}{3}\sum_\sigma \sigma^2 \left[(J_+^3 + J_-^3)\frac{2f_2(1-f_1)}{(\epsilon_2-\epsilon_1)(-\epsilon_1)} + (J_+^2 J_- + J_-^2 J_+) \times \right.$$

$$\left. \left(\frac{2f_2(1-f_1)}{(\epsilon_2-\epsilon_1)(-\epsilon_1-I)} + \frac{2f_2 f_3}{\epsilon_2(\epsilon_3-I)} \right) \right]$$

$$= \frac{2}{3}\left[(J_+^3 + J_-^3)\ln^2\frac{I}{D} + 2(J_+^2 J_- + J_-^2 J_+)\ln\frac{I}{D}\ln\frac{I}{D} + (J_+^2 J_- + J_-^2 J_+)\ln^2\frac{I}{D} \right]$$

Fourth order diagrams

a) Diagrams contributing to $J_+^4 + J_-^4$.

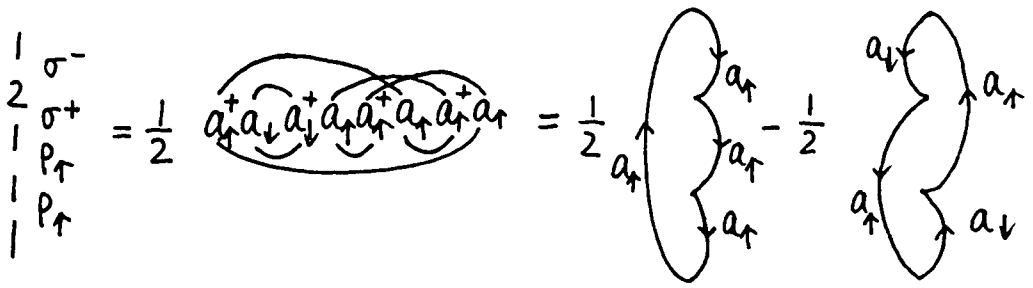

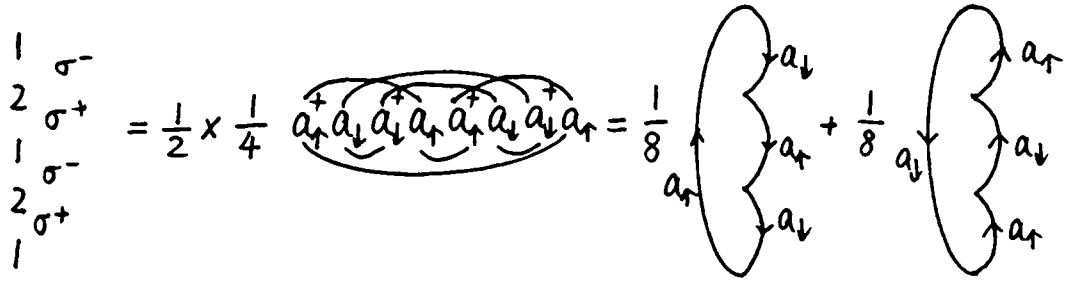

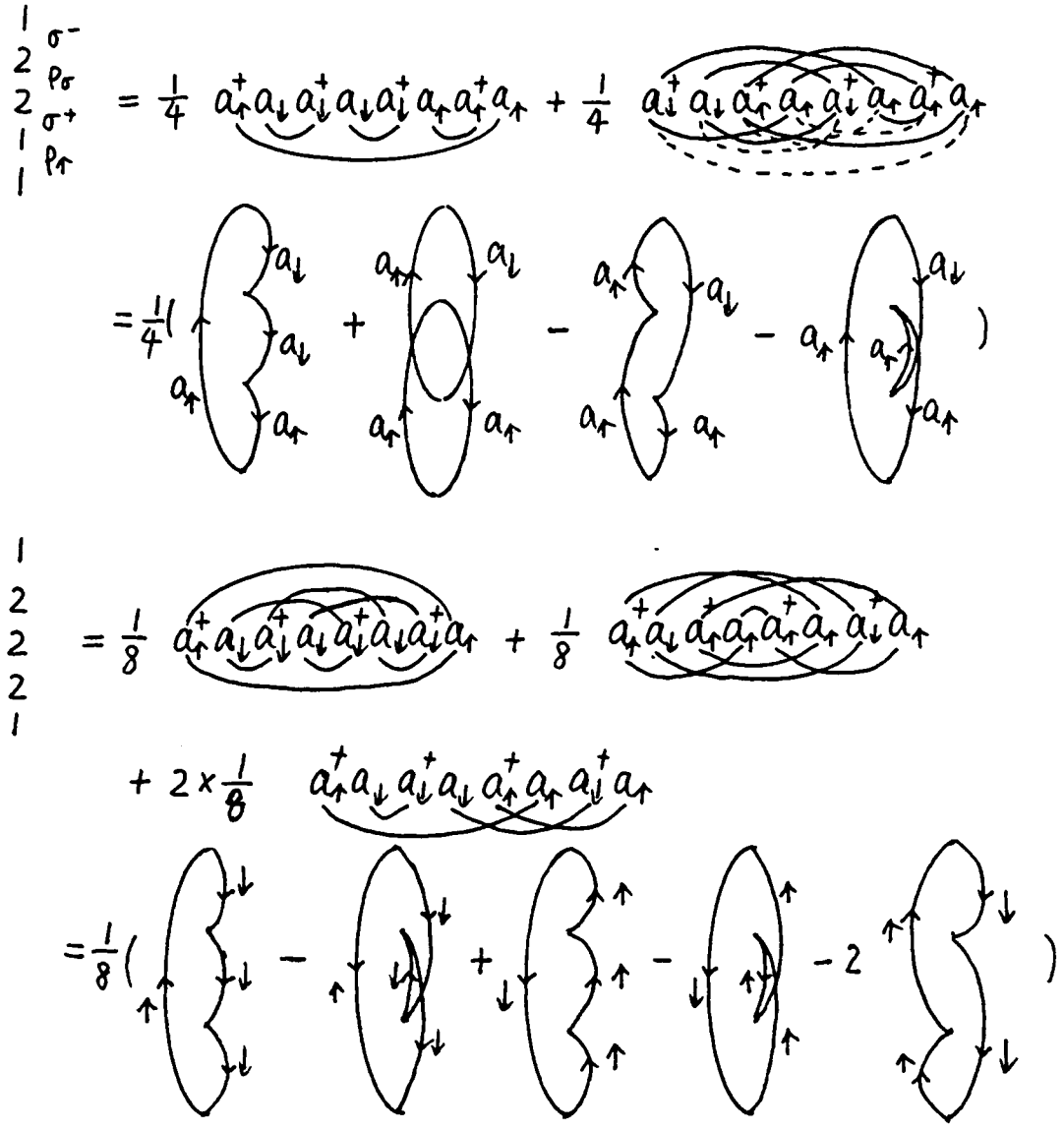

$$Z = \frac{e^{\beta I/2}}{2}\sum_{\sigma k} n_\sigma^2 (J_+^4 + J_-^4)\left(\frac{-\beta}{2\pi i}\right)\int d\zeta\, \frac{e^{-\beta\zeta}}{\zeta}\left[\frac{(1-f_1)f_2f_3f_4}{(\zeta+\epsilon_2-\epsilon_1)(\zeta+\epsilon_3-\epsilon_1)(\zeta+\epsilon_4-\epsilon_1-2\sigma H)}\right.$$

$$\left. - \frac{e^{\beta I/2}}{2}\sum_{\sigma k} n_\sigma^2 (J_+^4 + J_-^4)\left(\frac{-\beta}{2\pi i}\right)\int d\zeta\, \frac{e^{-\beta\zeta}}{\zeta}\left[\frac{(1-f_1)(1-f_2)f_3f_4}{(\zeta+\epsilon_3-\epsilon_1)(\zeta+\epsilon_3-\epsilon_2)(\zeta+\epsilon_4-\epsilon_2-2\sigma H)}\right]\right.$$

$$= -\frac{\beta e^{\beta I/2}}{2}\sum_{\sigma k} n_\sigma^2 (J_+^4 + J_-^4)\left[\frac{3(1-f_1)f_2f_3f_4}{(\epsilon_2-\epsilon_1)(\epsilon_3-\epsilon_1)(\epsilon_4-\epsilon_1+\sigma H)} - \frac{2(1-f_1)(1-f_2)f_3f_4}{(\epsilon_3-\epsilon_1)(\epsilon_4-\epsilon_1)(\epsilon_4-\epsilon_2-2\sigma H)}\right.$$

$$\left. - \frac{(1-f_3)(1-f_2)f_1f_4}{(\epsilon_1-\epsilon_3)(\epsilon_4-\epsilon_3)(\epsilon_1-\epsilon_3+\epsilon_4-\epsilon_2-2\sigma H)}\right]$$

$$\chi = \frac{1}{\beta}\frac{\partial^2}{\partial H^2}\frac{Z}{Z_0} = \frac{4}{3}\beta\sum_{\sigma k}\sigma^2 (J_+^4 + J_-^4)\left[\frac{3(1-f_1)f_2f_3}{(\epsilon_2-\epsilon_1)(\epsilon_3-\epsilon_1)(-\epsilon_1)} - \frac{2(1-f_1)f_3f_4}{(\epsilon_3-\epsilon_1)(\epsilon_4-\epsilon_1)\epsilon_4}\right.$$

$$\left. - \frac{f_1f_4(1-f_3)}{(\epsilon_1-\epsilon_3)(\epsilon_4-\epsilon_3)(\epsilon_1-\epsilon_3+\epsilon_4)}\right]$$

$$= \frac{2}{3}\beta (J_+^4 + J_-^4)\left(1 - \frac{1}{3} - 0\right) l_n^3 T/D$$

$$Z = -\frac{\beta e^{\beta I/2}}{8}\sum_{\sigma k} n_\sigma^2 (J_+^4 + J_-^4)\frac{1}{2\pi i}\int d\zeta\, \frac{e^{-\beta\zeta}}{\zeta}\left[\frac{(1-f_1)f_2f_3f_4}{(\zeta+\epsilon_2-\epsilon_1-2\sigma H)(\zeta+\epsilon_3-\epsilon_1)(\zeta+\epsilon_4-\epsilon_1-2\sigma H)}\right.$$

$$\left. + \frac{f_1(1-f_2)(1-f_3)(1-f_4)}{(\zeta+\epsilon_1-\epsilon_2-2\sigma H)(\zeta+\epsilon_1-\epsilon_3)(\zeta+\epsilon_1-\epsilon_4-2\sigma H)}\right]$$

$$= -\frac{\beta e^{\beta I/2}}{4}\sum_{\sigma k} n_\sigma^2 (J_+^4 + J_-^4)\left[\frac{(1-f_1)f_2f_3f_4}{(\epsilon_2-\epsilon_1-2\sigma H)(\epsilon_3-\epsilon_1)(\epsilon_4-\epsilon_1-2\sigma H)} + \frac{f_1(1-f_2)(1-f_3)(1-f_4)}{(\epsilon_1-\epsilon_2-2\sigma H)(\epsilon_1-\epsilon_3)(\epsilon_1-\epsilon_4-2\sigma H)}\right]$$

$$\chi = \frac{1}{\beta}\frac{\partial^2}{\partial H^2}\frac{Z}{Z_0} = \frac{4\beta}{3}\sum_{\sigma k}\sigma^2 (J_+^4 + J_-^4)\frac{2(1-f_1)f_2f_3}{(-\epsilon_1)(\epsilon_3-\epsilon_1)(\epsilon_2-\epsilon_1)} = \frac{2\beta}{3}(J_+^4 + J_-^4)\times\frac{2}{3} l_n^3 T/D$$

$$Z = \frac{e^{\beta\mathcal{Y}/2}}{4} \sum_{\sigma k} n_\sigma^2 (J_+^4 + J_-^4)\left(\frac{-\beta}{2\pi i}\right) \int d\zeta \, \frac{e^{-\beta\zeta}}{\zeta} \left[\frac{(1-f_k) f_2 f_3 f_4}{(\zeta+\epsilon_2-\epsilon_1)(\zeta+\epsilon_3-\epsilon_1-2\sigma H)(\zeta+\epsilon_4-\epsilon_1-2\sigma H)} \right.$$

$$- \frac{(1-f_1)(1-f_2) f_3 f_4}{(\zeta+\epsilon_3-\epsilon_1)(\zeta+\epsilon_4-\epsilon_1-2\sigma H)(\zeta+\epsilon_4-\epsilon_2-2\sigma H)} - \left. \frac{(1-f_1)(1-f_2) f_3 f_4}{(\zeta+\epsilon_3-\epsilon_1)(\zeta+\epsilon_4-\epsilon_1+\epsilon_3-\epsilon_2-2\sigma H)(\zeta+\epsilon_4-\epsilon_1-2\sigma H)} \right]$$

$$= -\frac{\beta e^{\beta\mathcal{Y}/2}}{2} \sum_{\sigma k} n_\sigma^2 (J_+^4 + J_-^4) \left[\frac{(1-f_1) f_2 f_3 f_4}{(\epsilon_2-\epsilon_1)(\epsilon_3-\epsilon_1-2\sigma H)(\epsilon_4-\epsilon_1-2\sigma H)} - \frac{(1-f_1)(1-f_2) f_3 f_4}{(\epsilon_3-\epsilon_1)(\epsilon_4-\epsilon_1-2\sigma H)(\epsilon_4-\epsilon_2-2\sigma H)} \right.$$

$$\left. - \frac{(1-f_1)(1-f_2) f_3 f_4}{(\epsilon_3-\epsilon_1)(\epsilon_3+\epsilon_4-\epsilon_1-\epsilon_2-2\sigma H)(\epsilon_4-\epsilon_1-2\sigma H)} \right]$$

$$\chi = \frac{1}{\beta} \frac{\partial^2}{\partial H^2} \mathcal{Z}/\mathcal{Z}_0 = \frac{4\beta}{3} \sum_\sigma \sigma^2 (J_+^4 + J_-^4) \left[\frac{2 f_2 f_3 (1-f_1)}{(\epsilon_2-\epsilon_1)(\epsilon_3-\epsilon_1)(-\epsilon_1)} - \frac{(1-f_1)(1-f_2) f_3}{(\epsilon_3-\epsilon_1)\epsilon_1\epsilon_2} \right.$$

$$\left. - \frac{(1-f_1)(1-f_2) f_3}{(\epsilon_3-\epsilon_1)(\epsilon_3-\epsilon_2-\epsilon_1)(-\epsilon_1)} \right]$$

$$= \frac{2\beta}{3} (J_+^4 + J_-^4) \left(\frac{2}{3} - \frac{1}{2} - \frac{1}{6} \right) \ln^3 T/D = 0$$

$$Z = \frac{e^{\beta\mathcal{Y}/2}}{8} \sum_{\sigma k} n_\sigma^2 (J_+^4 + J_-^4)\left(\frac{-\beta}{2\pi i}\right) \int d\zeta \, \frac{e^{-\beta\zeta}}{\zeta} \left[\frac{2(1-f_1) f_2 f_3 f_4}{(\zeta+\epsilon_2-\epsilon_1-2\sigma H)(\zeta+\epsilon_3-\epsilon_1-2\sigma H)(\zeta+\epsilon_4-\epsilon_1-2\sigma H)} \right.$$

$$- \frac{2(1-f_1)(1-f_2) f_3 f_4}{(\zeta+\epsilon_3-\epsilon_1-2\sigma H)(\zeta+\epsilon_3-\epsilon_1+\epsilon_4-\epsilon_2-2\sigma H)(\zeta+\epsilon_4-\epsilon_2-2\sigma H)} - \frac{2(1-f_1)(1-f_2) f_3 f_4}{(\zeta+\epsilon_3-\epsilon_1-2\sigma H)}$$

$$\left. \times \frac{1}{(\zeta+\epsilon_4-\epsilon_1-2\sigma H)(\zeta+\epsilon_4-\epsilon_2-2\sigma H)} \right]$$

$$= \frac{-\beta e^{\beta\mathcal{Y}/2}}{4} \sum_{\sigma k} n_\sigma^2 (J_+^4 + J_-^4) \left[\frac{(1-f_1) f_2 f_3 f_4}{(\epsilon_2-\epsilon_1-2\sigma H)(\epsilon_3-\epsilon_1-2\sigma H)(\epsilon_4-\epsilon_1-2\sigma H)} - \frac{(1-f_1)(1-f_2)}{(\epsilon_3-\epsilon_1-2\sigma H)} \right.$$

$$\times \frac{f_3 f_4}{(\epsilon_4-\epsilon_1-2\sigma H)(\epsilon_4-\epsilon_2-2\sigma H)} - \frac{(1-f_1)(1-f_2) f_3 f_4}{(\epsilon_3-\epsilon_1-2\sigma H)(\epsilon_3-\epsilon_1+\epsilon_4-\epsilon_2-2\sigma H)(\epsilon_4-\epsilon_2-2\sigma H)} \Big]$$

$$\chi = \frac{1}{\beta}\frac{\partial^2}{\partial H^2} Z/Z_0 = \frac{2\beta}{3} \sum_{\sigma k} \sigma^2 (J_+^4 + J_-^4) \Big[\frac{f_4 f_2 f_3}{\epsilon_4 \epsilon_2 \epsilon_3} - \frac{(1-f_2) f_3 f_4}{\epsilon_3 \epsilon_4 (\epsilon_3+\epsilon_4-\epsilon_2)}$$

$$- \frac{(1-f_2) f_3 f_4}{\epsilon_3 \epsilon_4 (\epsilon_4-\epsilon_2)} - \frac{(1-f_2) f_3 f_4}{(\epsilon_3-\epsilon_2)(\epsilon_4-\epsilon_2)\epsilon_4} \Big]$$

$$= \frac{2\beta}{3} (J_+^4 + J_-^4) \Big[\frac{1}{2} - \frac{1}{12} - \frac{1}{4} - \frac{1}{6} \Big] = 0$$

$$Z = \frac{e^{\beta I/2}}{4} \sum_{\sigma k} n\sigma^2 (J_+^4 + J_-^4) \left(\frac{-\beta}{2\pi i}\right) \int d\zeta \, \frac{e^{-\beta\zeta}}{\zeta} \Big[\frac{-2(1-f_1)(1-f_2) f_3 f_4}{(\zeta+\epsilon_3-\epsilon_1-2\sigma H)(\zeta+\epsilon_4-\epsilon_1-2\sigma H)}$$

$$\times \frac{1}{(\zeta+\epsilon_3-\epsilon_1+\epsilon_4-\epsilon_2-4\sigma H)} \Big]$$

$$= \frac{-\beta e^{\beta I/2}}{2} \sum_{\sigma k} n\sigma^2 (J_+^4 + J_-^4) \frac{-(1-f_1)(1-f_2) f_3 f_4}{(\epsilon_3-\epsilon_1-2\sigma H)(\epsilon_4-\epsilon_1-2\sigma H)(\epsilon_3+\epsilon_4-\epsilon_1-\epsilon_2-4\sigma H)}$$

$$\chi = \frac{1}{\beta}\frac{\partial^2}{\partial H^2} Z/Z_0 = \frac{4\beta}{3} \sum_{\sigma k} \sigma^2 (J_+^4 + J_-^4) \Big[\frac{-(1-f_2) f_3 f_4}{\epsilon_3 \epsilon_4 (\epsilon_3+\epsilon_4-\epsilon_2)} -$$

$$\frac{(1-f_1) f_3 f_4}{(\epsilon_3-\epsilon_1)(\epsilon_4-\epsilon_1)(\epsilon_3+\epsilon_4-\epsilon_1)} \Big]$$

$$= \frac{2\beta}{3} (J_+^4 + J_-^4) \left(-\frac{1}{3}\right) \ln^3 T/D$$

The total contribution to $J_+^4 + J_-^4$ is

$$\chi = \frac{2\beta}{3} (J_+^4 + J_-^4) \ln^3 T/D$$

b) diagrams Contributing to $J_+^3 J_- + J_-^3 J_+$

$$\begin{matrix}1\\0\\1\\1\\1\end{matrix}\ \begin{matrix}\sigma_{ab}^-\\ \sigma_{ab}^+\\ \rho_\uparrow\\ \rho_\uparrow\end{matrix} = \frac{1}{2}\, a_\uparrow^+ a_\uparrow a_\uparrow^+ a_\uparrow a_\uparrow^+ b_\downarrow b_\downarrow^+ a_\uparrow = \frac{1}{2}$$

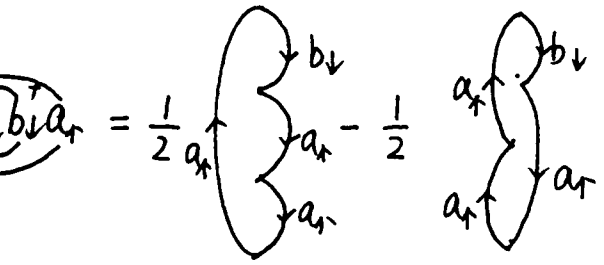

$$- \frac{1}{2}$$

$$\begin{matrix}1\\0\\1\\2\\1\end{matrix} = \frac{1}{4}\left\{ a_\uparrow^+ a_\downarrow a_\downarrow^+ a_\uparrow a_\uparrow^+ b_\downarrow b_\downarrow^+ a_\uparrow + a_\uparrow^+ a_\downarrow a_\downarrow^+ a_\uparrow b_\uparrow^+ a_\downarrow a_\downarrow^+ b_\uparrow \right\}$$

$$= \frac{1}{4}$$

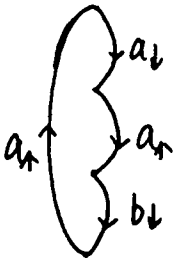

$$+ \frac{1}{4}$$

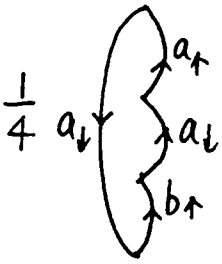

$$= \frac{1}{2}$$

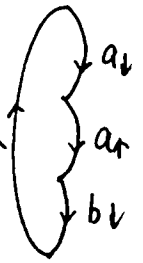

$$\begin{matrix}1 & 1\\0 & 2\\2 & 0\\1 & 1\\1 & 1\end{matrix} = 2 \times \frac{1}{4}\left(a_\uparrow^+ a_\uparrow a_\uparrow^+ a_\downarrow a_\downarrow^+ b_\downarrow b_\downarrow^+ a_\uparrow - a_\uparrow^+ a_\uparrow a_\uparrow^+ a_\downarrow b_\uparrow^+ a_\downarrow a_\downarrow^+ b_\uparrow \right)$$

$$= \frac{1}{2}$$

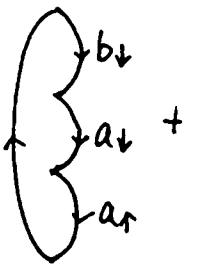

$$+ \frac{1}{2}$$

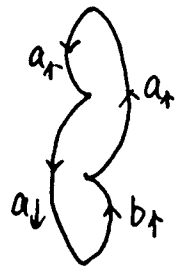

$$\begin{matrix}1\\2\\0\\2\\1\end{matrix} = \frac{1}{8}\left(a_\uparrow^+ a_\downarrow a_\uparrow^+ b_\downarrow b_\uparrow^+ a_\uparrow a_\downarrow^+ a_\uparrow + a_\uparrow^+ a_\downarrow b_\uparrow^+ a_\uparrow a_\uparrow^+ b_\uparrow a_\downarrow^+ a_\uparrow \right.$$

$$\left. + a_\uparrow^+ a_\downarrow a_\downarrow^+ b_\downarrow b_\downarrow^+ a_\downarrow a_\downarrow^+ a_\uparrow + a_\uparrow^+ a_\downarrow b_\downarrow^+ a_\downarrow a_\downarrow^+ b_\downarrow a_\downarrow^+ a_\uparrow \right)$$

$$\begin{matrix}1\\0\\1\\1\\1\end{matrix} + \begin{matrix}1\\0\\1\\2\\1\end{matrix} + \begin{matrix}1\\0\\2\\1\\1\end{matrix} + \begin{matrix}1\\2\\0\\2\\1\end{matrix} + \begin{matrix}1\\0\\0\\1\\1\end{matrix} + \begin{matrix}1\\0\\0\\0\\1\end{matrix}$$

$$Z = \frac{1}{2}\sum_{\sigma k} n_\sigma^2 e^{\beta I/2}(\bar{J}_+^3 J_- + \bar{J}_-^3 J_+) f_1 f_2 f_3 (1-f_4) \times \left(\frac{-\beta}{2\pi i}\right)\int d\zeta \ \frac{e^{-\beta\zeta}}{\zeta}$$

$$\left\{\frac{1}{(\zeta+\epsilon_1-\epsilon_4)(\zeta+\epsilon_2-\epsilon_4)(\zeta+\epsilon_3-\epsilon_4-2\sigma H-I)} + \frac{1}{(\zeta+\epsilon_1-\epsilon_4-2\sigma H)(\zeta+\epsilon_3-\epsilon_4-2\sigma H-I)}\right.$$

$$\times\frac{1}{(\zeta+\epsilon_2-\epsilon_4)} + \frac{1}{(\zeta+\epsilon_1-\epsilon_4)(\zeta+\epsilon_2-\epsilon_4-2\sigma H)(\zeta+\epsilon_3-\epsilon_4-2\sigma H-I)} + \frac{1}{2(\zeta+\epsilon_1-\epsilon_4-2\sigma H)}$$

$$\left.\times\frac{1}{(\zeta+\epsilon_2-\epsilon_4-2\sigma H-I)(\zeta+\epsilon_3-\epsilon_4-2\sigma H)} + \frac{1}{2(\zeta+\epsilon_1-\epsilon_4-2\sigma H-I)(\zeta+\epsilon_2-\epsilon_4-2\sigma H-I)(\zeta+\epsilon_3-\epsilon_4-2\sigma H-I)}\right\}$$

$$+\frac{1}{2}\sum_{\sigma k} n_\sigma^2 e^{\beta I/2}(\bar{J}_+^3 + \bar{J}_-^3 J_+) f_1 f_2 (1-f_3)(1-f_4) \times \left(\frac{-\beta}{2\pi i}\right)\int d\zeta \ \frac{e^{-\beta\zeta}}{\zeta}$$

$$\left\{\frac{-1}{(\zeta+\epsilon_1-\epsilon_3)(\zeta+\epsilon_2-\epsilon_3)(\zeta+\epsilon_2-\epsilon_4-2\sigma H-I)} + \frac{1}{(\zeta+\epsilon_1-\epsilon_3-2\sigma H-I)(\zeta+\epsilon_2-\epsilon_3-2\sigma H)(\zeta+\epsilon_2-\epsilon_4)}\right.$$

$$+\frac{-1}{2(\zeta+\epsilon_1-\epsilon_3-2\sigma H)(\zeta+\epsilon_1-\epsilon_3+\epsilon_2-\epsilon_4-2\sigma H-I)(\zeta+\epsilon_1-\epsilon_4-2\sigma H)} + \frac{-1}{2(\zeta+\epsilon_1-\epsilon_3-2\sigma H-I)}$$

$$\times\frac{1}{(\zeta+\epsilon_1-\epsilon_3+\epsilon_2-\epsilon_4-2\sigma H-I)(\zeta+\epsilon_1-\epsilon_4)} + \frac{-1-1}{4(\zeta+\epsilon_1-\epsilon_3-2\sigma H-I)(\zeta+\epsilon_1-\epsilon_3+\epsilon_2-\epsilon_4-2\sigma H-I)}$$

$$\left.\times\frac{1}{(\zeta+\epsilon_1-\epsilon_4-2\sigma H-I)} + \frac{-1}{2(\zeta+\epsilon_1-\epsilon_4)(\zeta+\epsilon_1-\epsilon_3-2\sigma H-I)(\zeta+\epsilon_2-\epsilon_3-2\sigma H-I)}\right\}$$

$$= \frac{-\beta}{2}\sum_{\sigma k} n_\sigma^2 e^{\beta I/2}(\bar{J}_+^3 J_- + \bar{J}_-^3 J_+) f_1 f_2 f_3 (1-f_4)\left\{\frac{3}{(\epsilon_1-\epsilon_4)(\epsilon_2-\epsilon_4)(\epsilon_3-\epsilon_4-2\sigma H-I)}\right.$$

$$+\frac{2+2}{(\epsilon_1-\epsilon_4-2\sigma H)(\epsilon_2-\epsilon_4)(\epsilon_3-\epsilon_4-2\sigma H-I)}+\frac{1}{2(\epsilon_1-\epsilon_4-2\sigma H)(\epsilon_2-\epsilon_4-2\sigma H-I)(\epsilon_3-\epsilon_4-2\sigma H)}$$

$$+\frac{1}{2(\epsilon_1-\epsilon_4-2\sigma H-I)(\epsilon_2-\epsilon_4-2\sigma H-I)(\epsilon_3-\epsilon_4-2\sigma H-I)}\Big\}+\frac{-\beta}{2}\sum_{\sigma k} n_\sigma^2 e^{\beta I/2}(\bar{J}_+^3 J_-+\bar{J}_-^3 J_+)$$

$$f_1 f_2 (1-f_3)(1-f_4)\Big\{\frac{-1}{(\epsilon_1-\epsilon_3)(\epsilon_2-\epsilon_3)(\epsilon_1+\epsilon_2-\epsilon_3-\epsilon_4-2\sigma H-I)}+\frac{-2}{(\epsilon_1-\epsilon_3)(\epsilon_2-\epsilon_3)}$$

$$\times\frac{1}{(\epsilon_2-\epsilon_4-2\sigma H-I)}+\frac{1}{(\epsilon_2-\epsilon_4)(\epsilon_1-\epsilon_3-2\sigma H-I)(\epsilon_1-\epsilon_3-2\sigma H)}+\frac{1}{(\epsilon_2-\epsilon_4)(\epsilon_1+\epsilon_2-\epsilon_3-\epsilon_4-2\sigma H-I)}$$

$$\times\frac{1}{(\epsilon_2-\epsilon_3)}+\frac{-1}{2(\epsilon_1-\epsilon_3-2\sigma H)(\epsilon_1-\epsilon_3+\epsilon_2-\epsilon_4-2\sigma H-I)(\epsilon_1-\epsilon_4-2\sigma H)}+\frac{-1}{2(\epsilon_1-\epsilon_3-2\sigma H-I)}$$

$$\times\frac{1}{(\epsilon_1-\epsilon_3+\epsilon_2-\epsilon_4-2\sigma H-I)(\epsilon_1-\epsilon_4)}+\frac{-1}{2(\epsilon_1-\epsilon_3-2\sigma H-I)(\epsilon_2-\epsilon_3-2\sigma H-I)(\epsilon_1-\epsilon_4)}+$$

$$\frac{-2}{4(\epsilon_1-\epsilon_3-2\sigma H-I)(\epsilon_1-\epsilon_3+\epsilon_2-\epsilon_4-2\sigma H-I)(\epsilon_1-\epsilon_4-2\sigma H-I)}+\frac{-1}{2(\epsilon_1-\epsilon_4)(\epsilon_1-\epsilon_3-2\sigma H-I)(\epsilon_2-\epsilon_3-2\sigma H-I)}\Big\}$$

$$\chi=\frac{1}{\beta}\frac{\partial^2}{\partial H^2}Z/Z_0=\frac{4\beta}{3}\sum_{\sigma k}\sigma^2(\bar{J}_+^3 J_-+\bar{J}_-^3 J_+)\Big\{\frac{3f_1f_2(1-f_4)}{(\epsilon_1-\epsilon_4)(\epsilon_2-\epsilon_4)(-\epsilon_4-I)}+$$

$$\frac{(2+\frac{1}{2})f_1f_2f_3}{\epsilon_1\epsilon_2(\epsilon_3-I)}+\frac{2f_1f_2(1-f_4)}{(\epsilon_1-\epsilon_4)(\epsilon_2-\epsilon_4)(-\epsilon_4-I)}+\frac{f_1f_2f_3}{2(\epsilon_1-I)(\epsilon_2-I)(\epsilon_3-I)}\Big\}+\frac{4\beta}{3}\sum_{\sigma k}\sigma^2$$

$$(\bar{J}_+^3 J_-+\bar{J}_-^3 J_+)\times\Big\{\frac{-f_1f_2(1-f_3)}{(\epsilon_1-\epsilon_3)(\epsilon_2-\epsilon_3)(\epsilon_1+\epsilon_2-\epsilon_3-I)}+\frac{-2f_1f_2(1-f_3)}{(\epsilon_1-\epsilon_3)(\epsilon_2-\epsilon_3)(\epsilon_2-I)}+\frac{f_1f_2(1-f_4)}{(\epsilon_2-\epsilon_4)(\epsilon_1-I)\epsilon_2}$$

$$+\frac{f_2(1-f_3)(1-f_4)}{(\epsilon_2-\epsilon_4)(\epsilon_2-\epsilon_3)(\epsilon_2-\epsilon_3-\epsilon_4-I)}+\frac{-f_2(1-f_3)(1-f_4)}{2(-\epsilon_3)(\epsilon_2-\epsilon_3-\epsilon_4-I)(-\epsilon_4-I)}+\frac{-f_1f_2(1-f_4)}{2(\epsilon_1-I)(\epsilon_1-\epsilon_4)(\epsilon_1+\epsilon_2-\epsilon_4-I)}$$

$$+\frac{-f_1f_2(1-f_4)}{2(\epsilon_1-I)(\epsilon_2-I)(\epsilon_1-\epsilon_4)}+\frac{-f_2(1-f_3)(1-f_4)}{2(-\epsilon_3-I)(\epsilon_2-\epsilon_3-\epsilon_4-I)(-\epsilon_4-I)}+\frac{-f_1f_2(1-f_4)}{2(\epsilon_1-\epsilon_4)(\epsilon_1-I)(\epsilon_2-I)}\Big\}$$

$$= \frac{4\beta}{3} \sum_{\sigma} \sigma^2 (\bar{J}_+^3 J_- + \bar{J}_-^3 J_+) \Big\{ \ln^3 I/D + \frac{5}{2} \ln^2 I/D \ln I/D + \frac{2}{3} \ln^3 I/D + \frac{1}{2} \ln^3 I/D \Big\}$$

$$+ \frac{4\beta}{3} \sum_{\sigma} \sigma^2 (\bar{J}_+^3 J_- + \bar{J}^3 J_+) \Big\{ 0 - \frac{1}{3} \ln^3 I/D + \frac{1}{2} \ln^2 I/D \ln I/D + 0 - \frac{1}{12} \ln^3 I/D$$

$$- \frac{1}{6} \ln^3 I/D - \frac{1}{4} \ln^3 I/D - \frac{1}{12} \ln^3 I/D - \frac{1}{4} \ln^3 I/D \Big\}$$

The total contribution to $J_+^2 J_- + J_-^2 J_+$ is

$$\chi = \frac{2}{3} (\bar{J}_+^3 J_- + \bar{J}_-^3 J_+) (3 \ln^2 T/D \ln I/D + \ln^3 I/D)$$

c) diagrams contributing to $J_+^2 J_-^2$

$$\begin{matrix} 1 \\ 0 \\ 0 \\ 1 \\ 1 \end{matrix} = \frac{1}{4} \; \underbrace{a_\uparrow^+ a_\uparrow \, a_\uparrow^+ b_\downarrow \, b_\downarrow^+ b_\downarrow \, b_\downarrow^+ a_\uparrow}$$

$= \frac{1}{4}$

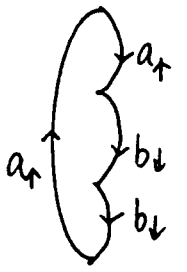

$$\begin{matrix}1\\0\\3\\2\\1\end{matrix} \;+\; \begin{matrix}1\\2\\3\\0\\1\end{matrix} \;=\; 2\times\frac{1}{4}\left\{\begin{matrix}-b_\uparrow b_\downarrow a_\uparrow a_\downarrow a_\downarrow a\, b_\downarrow a_\uparrow\\ -a_\uparrow^+ a_\downarrow b_\uparrow^+ b_\downarrow a_\downarrow^+ b_\uparrow b_\downarrow^+ a_\uparrow\end{matrix}\right\} =$$

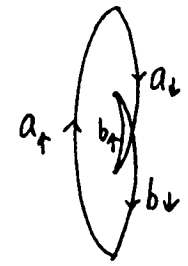

$$\begin{matrix}1\\0\\3\\0\\1\end{matrix} \;=\; \frac{1}{4}\; a_\uparrow^+ b_\downarrow a_\uparrow^+ b_\downarrow b_\downarrow^+ a_\uparrow b_\downarrow^+ a_\uparrow \;=\; -\frac{1}{2}$$

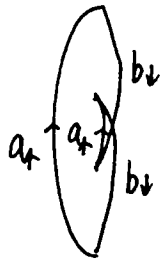

$$\begin{matrix}1\\0\\0\\0\\1\end{matrix} \;=\; \frac{1}{8}\left\{\begin{matrix}a_\uparrow^+ b_\downarrow a_\uparrow^+ a_\uparrow b_\downarrow^+ b_\downarrow b_\downarrow^+ a_\uparrow\\ a_\uparrow^+ b_\downarrow b_\downarrow^+ b_\downarrow a_\uparrow^+ a_\uparrow b_\downarrow^+ a_\uparrow\end{matrix}\right\} = -\frac{1}{4}$$

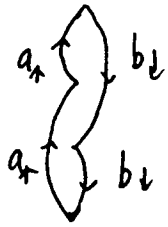

$$\begin{matrix}1\\0\\2\\2\\1\end{matrix} \;+\; \begin{matrix}1\\2\\2\\0\\1\end{matrix} \;=\; 2\times\frac{1}{8}\left\{\begin{matrix}a_\uparrow^+ b_\downarrow b_\downarrow^+ a_\downarrow b_\downarrow^+ b_\downarrow a_\downarrow^+ a_\uparrow\\ -b_\uparrow^+ a_\downarrow a_\uparrow^+ b_\uparrow b_\uparrow^+ b_\uparrow a_\uparrow^+ a_\uparrow\end{matrix}\right\} = 0$$

$$\begin{matrix}1\\2\\0\\0\\1\end{matrix} \;+\; \begin{matrix}1\\0\\0\\2\\1\end{matrix} \;=\; 2\times\frac{1}{8}\left\{\begin{matrix}a_\uparrow^+ b_\downarrow b_\downarrow^+ b_\downarrow b_\downarrow^+ a_\downarrow a_\downarrow^+ a_\uparrow\\ -b_\uparrow^+ a_\downarrow b_\uparrow^+ b_\uparrow a_\uparrow^+ b_\uparrow a_\downarrow^+ a_\uparrow\end{matrix}\right\} = 0$$

$= \frac{1}{8}\Big(-$ 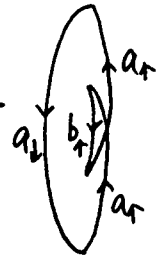 $-$ 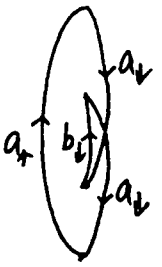 $+$ 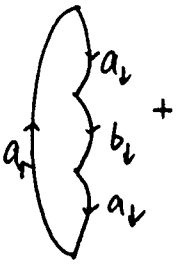 $+$ 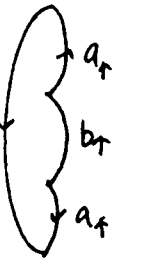 $\Big)$

1 2 2 0 1

$= \frac{1}{8}\Big($ $a^+_\uparrow b_\downarrow b^+_\downarrow a_\downarrow a^+_\downarrow a_\downarrow a^+_\downarrow a_\uparrow$ $+$ $a^+_\uparrow b_\downarrow b^+_\downarrow a_\downarrow a^+_\uparrow a_\uparrow a^+_\downarrow a_\uparrow$

$- b^+_\uparrow a_\downarrow a^+_\uparrow b_\uparrow a^+_\downarrow a_\downarrow a^+_\downarrow a_\uparrow$ $-$ $b^+_\uparrow a_\downarrow a^+_\uparrow b_\uparrow a^+_\uparrow a_\uparrow a^+_\downarrow a_\uparrow$ $\Big)$

$= \frac{1}{8}\Big($ 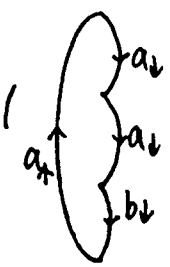 $-$ 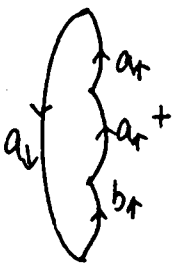 $+$  $-$ 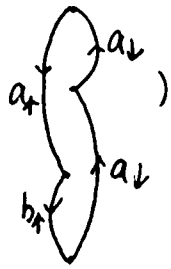 $\Big)$

$= 0$

1 0 0 1 1

$= \frac{1}{4}$ $a^+_\uparrow a_\uparrow a^+_\uparrow b_\downarrow a^+_\uparrow a_\uparrow b^+_\downarrow a_\uparrow$ $= \frac{1}{4}\Big\{-$ 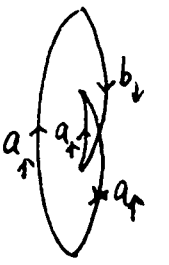 $-$ 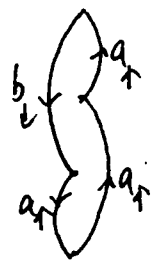 $\Big)$

1 0 0 0 1

$= \frac{1}{8}\Big($ $a^+_\uparrow b_\downarrow a^+_\uparrow a_\uparrow a^+_\uparrow a_\uparrow b^+_\downarrow a_\uparrow$

$b^+_\uparrow a_\downarrow a^+_\downarrow a_\downarrow a^+_\downarrow a_\downarrow a^+_\downarrow b_\uparrow$ $\Big) = \frac{1}{4}\Big\{$ 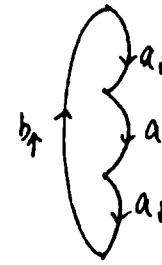 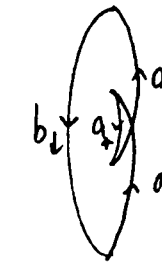 $\Big\}$

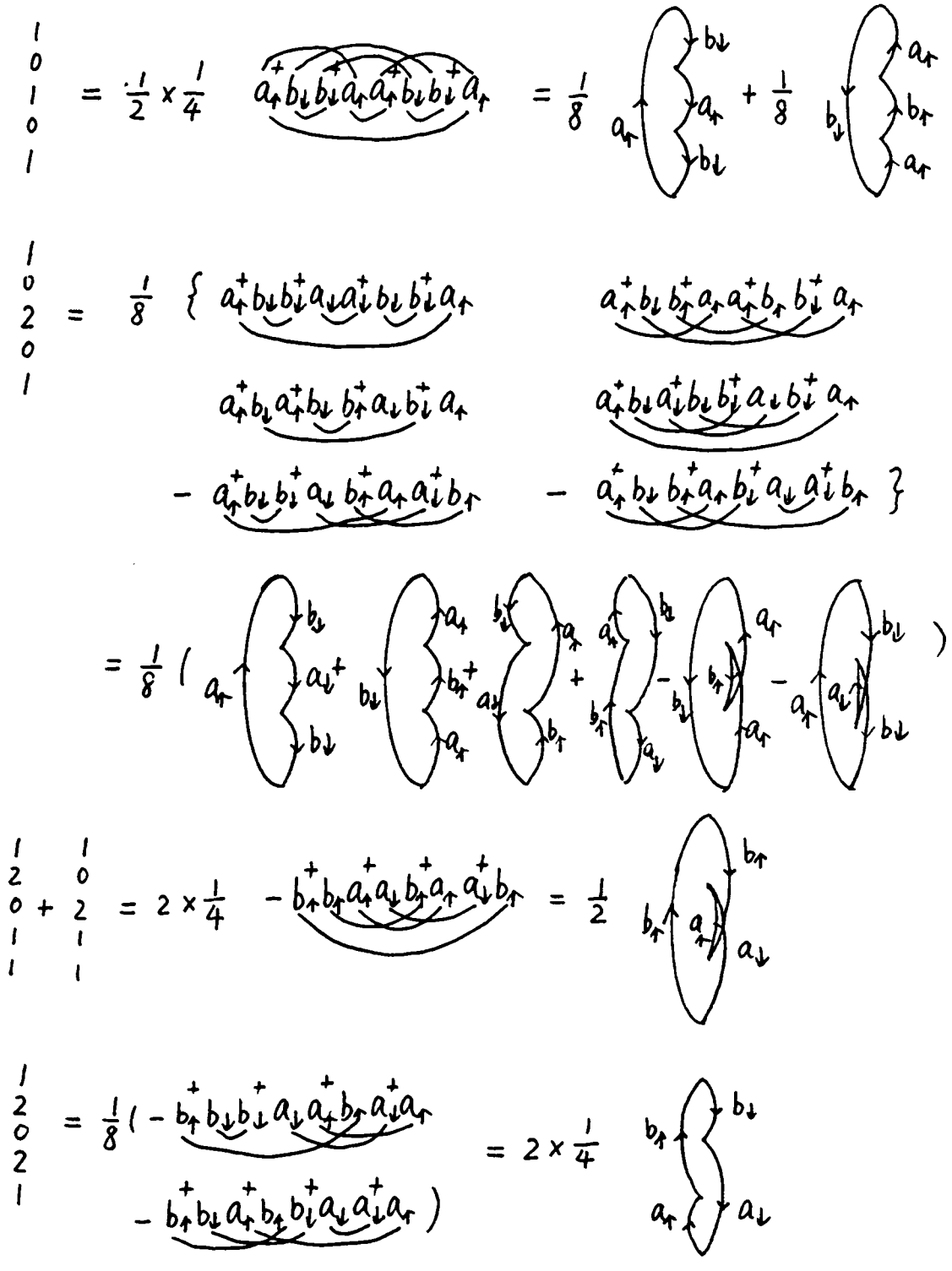

$$\begin{matrix}1\\0\\0\\1\\1\end{matrix}+\begin{matrix}1\\0\\1\\0\\1\end{matrix}+\begin{matrix}1\\0\\2\\0\\1\end{matrix}+\begin{matrix}1\\0\\3\\0\\1\end{matrix}$$

$$Z=\frac{1}{4}\sum_{\sigma k} n_\sigma^2 e^{\beta I/2}(J_+^2J_-^2+J_-^2J_+^2)f_1(1-f_2)(1-f_3)(1-f_4)$$

$$\times\left(\frac{-\beta}{2\pi i}\right)\int d\zeta\ \frac{e^{-\beta\zeta}}{\zeta}\left\{\frac{1}{(\zeta+\epsilon_1-\epsilon_2)(\zeta+\epsilon_1-\epsilon_3-2\sigma H-I)(\zeta+\epsilon_1-\epsilon_4-2\sigma H-I)}+\frac{1}{(\zeta+\epsilon_1-\epsilon_2-2\sigma H-I)}\right.$$

$$\left.\times\frac{1}{(\zeta+\epsilon_1-\epsilon_3)(\zeta+\epsilon_1-\epsilon_4-2\sigma H-I)}+\frac{1}{(\zeta+\epsilon_1-\epsilon_2-2\sigma H-I)(\zeta+\epsilon_1-\epsilon_3-2\sigma H)(\zeta+\epsilon_1-\epsilon_4-2\sigma H-I)}\right\}$$

$$+\frac{\beta}{4}\sum_{\sigma k} n_\sigma^2 e^{\beta I/2}(J_+^2J_-^2+J_-^2J_+^2)f_1f_2(1-f_3)(1-f_4)\left(\frac{-\beta}{2\pi i}\right)\int d\zeta\ \frac{e^{-\beta I}}{\zeta}\left\{\frac{-3}{(\zeta+\epsilon_1-\epsilon_3-2\sigma H-I)}\right.$$

$$\left.\times\frac{1}{(\zeta+\epsilon_1-\epsilon_3+\epsilon_2-\epsilon_4-2\sigma H)(\zeta+\epsilon_1-\epsilon_4-2\sigma H-I)}+\frac{}{(\zeta+\epsilon_1-\epsilon_3-2\sigma H-I)(\zeta+\epsilon_1-\epsilon_4-2\sigma H)(\zeta+\epsilon_2-\epsilon_4-2\sigma H-I)}\right\}$$

$$=\frac{-\beta}{2}\sum_{\sigma k} n_\sigma^2 e^{\beta I/2}(J_+^2J_-^2+J_-^2J_+^2)f_1(1-f_2)(1-f_3)(1-f_4)\left\{\frac{2}{(\epsilon_1-\epsilon_2)(\epsilon_1-\epsilon_3-2\sigma H-I)(\epsilon_1-\epsilon_4-2\sigma H-I)}\right.$$

$$\left.+\frac{1/2}{(\epsilon_1-\epsilon_2-2\sigma H-I)(\epsilon_1-\epsilon_3-2\sigma H)(\epsilon_1-\epsilon_4-2\sigma H-I)}\right\}+\frac{-\beta}{4}\sum_{\sigma k} n_\sigma^2 e^{\beta I/2}(J_+^2J_-^2+J_-^2J_+^2)$$

$$\times f_1f_2(1-f_3)(1-f_4)\left\{\frac{-3}{(\epsilon_1-\epsilon_3-2\sigma H-I)(\epsilon_1-\epsilon_3+\epsilon_2-\epsilon_4-2\sigma H)(\epsilon_1-\epsilon_4-2\sigma H-I)}+\right.$$

$$\left.\frac{1}{(-I+\epsilon_1-\epsilon_3-2\sigma H)(\epsilon_1-\epsilon_4-2\sigma H)(\epsilon_2-\epsilon_4-2\sigma H-I)}\right\}$$

$$\chi=\frac{1}{\beta}\frac{\partial^2}{\partial H^2}Z/Z_0=\frac{4\beta}{3}\sum_\sigma \sigma^2(J_+^2J_-^2+J_-^2J_+^2)\left\{\frac{f_1(1-f_2)(1-f_3)\times 4}{(\epsilon_1-\epsilon_2)(\epsilon_1-\epsilon_3-I)(\epsilon_4-I)}+\frac{(1-f_2)(1-f_3)}{2(-\epsilon_2)(-\epsilon_3-I)}\right.$$

$$\left.\times\frac{(1-f_4)}{(-\epsilon_4-I)}+\frac{-3f_2(1-f_3)(1-f_4)}{2(\epsilon_3-I)(\epsilon_2-\epsilon_3-\epsilon_4-I)(-\epsilon_4-I)}+\frac{f_1f_2(1-f_3)}{2(\epsilon_1-\epsilon_3-I)\epsilon_1(\epsilon_2-I)}\right.$$

$$+\frac{f_1 f_2 (1-f_4)}{2\epsilon_1(\epsilon_1-\epsilon_4)(\epsilon_2-\epsilon_4-I)}\Big\} = \frac{2\beta}{3}(J_+^2J_-^2+J_-^2J_+)\Big(\frac{4}{3}\ln^3 I/D + \frac{1}{2}\ln T/D \ln^2 I/D$$

$$-\frac{1}{2}\ln^3 I/D + \frac{1}{2}\ln^2 I/D\,(\ln T/D - \frac{1}{2}\ln I/D) + \frac{1}{12}\ln I/D\Big)$$

$$= \frac{2\beta}{3}(J_+^2J_-^2+J_-^2J_+^2)\Big(\ln T/D \ln^2 I/D + \frac{2}{3}\ln^3 I/D\Big)$$

$$\begin{array}{ccccccc} 1 & & 1 & & 1 & & 1 \\ 2 & & 0 & & 0 & & 0 \\ 0 & + & 2 & + & 3 & + & 0 \\ 2 & & 1 & & 2 & & 0 \\ 1 & & 1 & & 1 & & 1 \end{array}$$

$$Z = \frac{1}{4}\sum_{\sigma k} n_\sigma^2 e^{\beta I/2}(J_+^2J_-^2+J_-^2J_+)\,f_1 f_2 (1-f_3)(1-f_4)\Big(\frac{-\beta}{2\pi i}\Big)\int d\zeta\, \frac{e^{-\beta\zeta}}{\zeta}$$

$$\Big\{\frac{1}{(\zeta+\epsilon_1-\epsilon_3-2\sigma H)(\zeta+\epsilon_2-\epsilon_3-2\sigma H-I)(\zeta+\epsilon_2-\epsilon_4-2\sigma H)} + \frac{2}{(\zeta+\epsilon_1-\epsilon_3)(\zeta+\epsilon_1-\epsilon_3+\epsilon_2-\epsilon_4-2\sigma H)}$$

$$\times\frac{}{(\zeta+\epsilon_1-\epsilon_4-2\sigma H-I)} + \frac{4}{(\zeta+\epsilon_1-\epsilon_3-2\sigma H-I)(\zeta+\epsilon_1-\epsilon_3+\epsilon_2-\epsilon_4-2\sigma H)(\zeta+\epsilon_1-\epsilon_4-2\sigma H)}$$

$$+\frac{-1}{(\zeta+\epsilon_1-\epsilon_3-2\sigma H-I)(\zeta+\epsilon_1-\epsilon_4-2\sigma H-I)(\zeta+\epsilon_2-\epsilon_4-2\sigma H-I)}\Big\}$$

$$= \frac{-\beta}{2}\sum_{\sigma k} n_\sigma^2 e^{\beta I/2}(J_+^2J_-^2+J_-^2J_+^2)\,f_1 f_2 (1-f_3)(1-f_4)\Big\{\frac{1/2}{(\epsilon_1-\epsilon_3-2\sigma H)(\epsilon_2-\epsilon_3-2\sigma H-I)}$$

$$\times\frac{1}{(\epsilon_2-\epsilon_4-2\sigma H)} + \frac{2}{(\epsilon_1-\epsilon_3-2\sigma H-I)(\epsilon_1+\epsilon_2-\epsilon_3-\epsilon_4-2\sigma H)}\Big(\frac{1}{(\epsilon_1-\epsilon_4-2\sigma H)} + \frac{1/2}{(\epsilon_1-\epsilon_4)}\Big)$$

$$+\frac{1}{(\epsilon_1-\epsilon_3)(\epsilon_2-\epsilon_4-2\sigma H)(\epsilon_1-\epsilon_4-2\sigma H-I)} + \frac{-1/2}{(\epsilon_1-\epsilon_3-2\sigma H-I)(\zeta+\epsilon_1-\epsilon_4-2\sigma H-I)(\zeta+\epsilon_2-\epsilon_4-2\sigma H-I)}\Big\}$$

$$\chi = \frac{4\beta}{3} \sum_{\sigma k} \sigma^2 (J_+^2 J_-^2 + J_-^2 J_+^2) \left\{ \frac{\frac{1}{2} f_1 f_2 (1-f_3)}{(\epsilon_1-\epsilon_3)(\epsilon_2-\epsilon_3-I)\epsilon_2} + \frac{\frac{1}{2} f_1 f_2 (1-f_4)}{\epsilon_1(\epsilon_2-I)(\epsilon_2-\epsilon_4)} \right.$$

$$+ \frac{2 f_2 (1-f_3)(1-f_4)}{(-\epsilon_4)(\epsilon_2-\epsilon_3-\epsilon_4)(-\epsilon_3-I)} + \frac{2 f_1 (1-f_3)(1-f_4)}{(\epsilon_1-I)(\epsilon_1-\epsilon_3-\epsilon_4)(\epsilon_1-\epsilon_4)} + \frac{f_1 f_2 (1-f_3)}{(\epsilon_1-\epsilon_3)\epsilon_2(\epsilon_1-I)}$$

$$\left. + \frac{-\frac{1}{2} f_1 f_2 (1-f_4)}{(\epsilon_1-\epsilon_4)(\epsilon_1-\epsilon_4-I)(\epsilon_2-\epsilon_4-I)} + \frac{-\frac{1}{2} f_1 f_2 (1-f_3)}{(\epsilon_1-\epsilon_3-I)(\epsilon_1-I)(\epsilon_2-I)} \right\}$$

$$= \frac{2\beta}{3}(J_+^2 J_-^2 + J_-^2 J_+^2) \left\{ \frac{1}{2} \ln^2 \frac{I}{D} \left(\frac{1}{2} \ln \frac{T}{D} - \frac{1}{3} \ln \frac{I}{D} \right) + \frac{1}{4} \ln^2 \frac{I}{D} \ln \frac{T}{D} + \left(\ln^2 \frac{I}{D} \ln \frac{T}{D} \right.\right.$$

$$\left.\left. - \frac{1}{3} \ln^3 \frac{I}{D} \right) + \frac{1}{6} \ln^3 \frac{I}{D} + \frac{1}{2} \ln^2 \frac{I}{D} \ln \frac{T}{D} - \frac{1}{3} \ln^3 \frac{I}{D} \right\}$$

$$= \frac{2\beta}{3} (J_+^2 J_-^2 + J_-^2 J_+^2) \left\{ 2 \ln^2 \frac{I}{D} \ln \frac{T}{D} - \frac{2}{3} \ln^3 \frac{I}{D} \right\}$$

The total contribution to $J_+^2 J_-^2$ is

$$\chi = \frac{2\beta}{3} (J_+^2 J_-^2 + J_-^2 J_+^2) \times 3 \ln^2 \frac{I}{D} \ln \frac{T}{D}$$

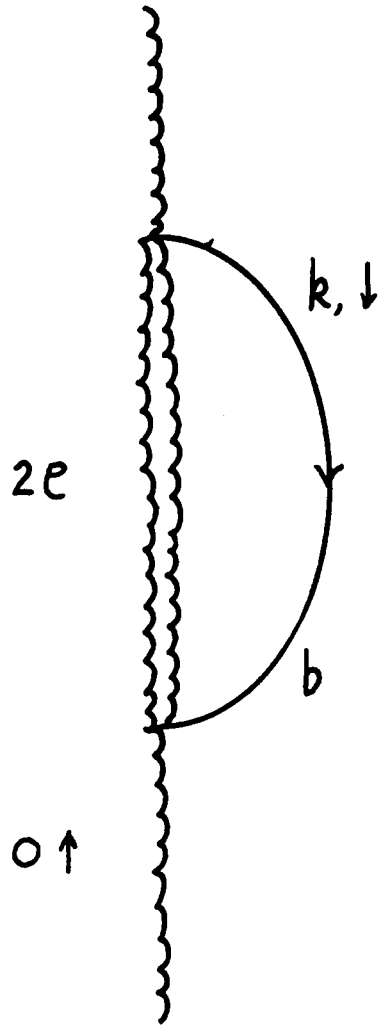

(a)

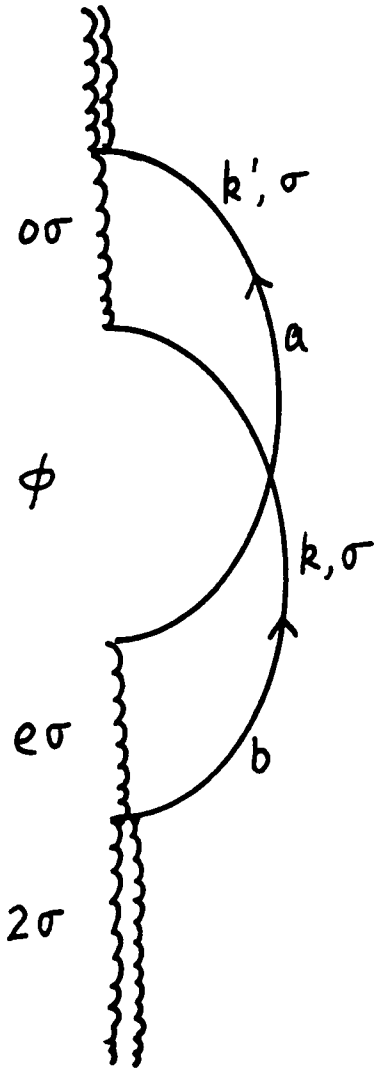

(b)

Fig. 1

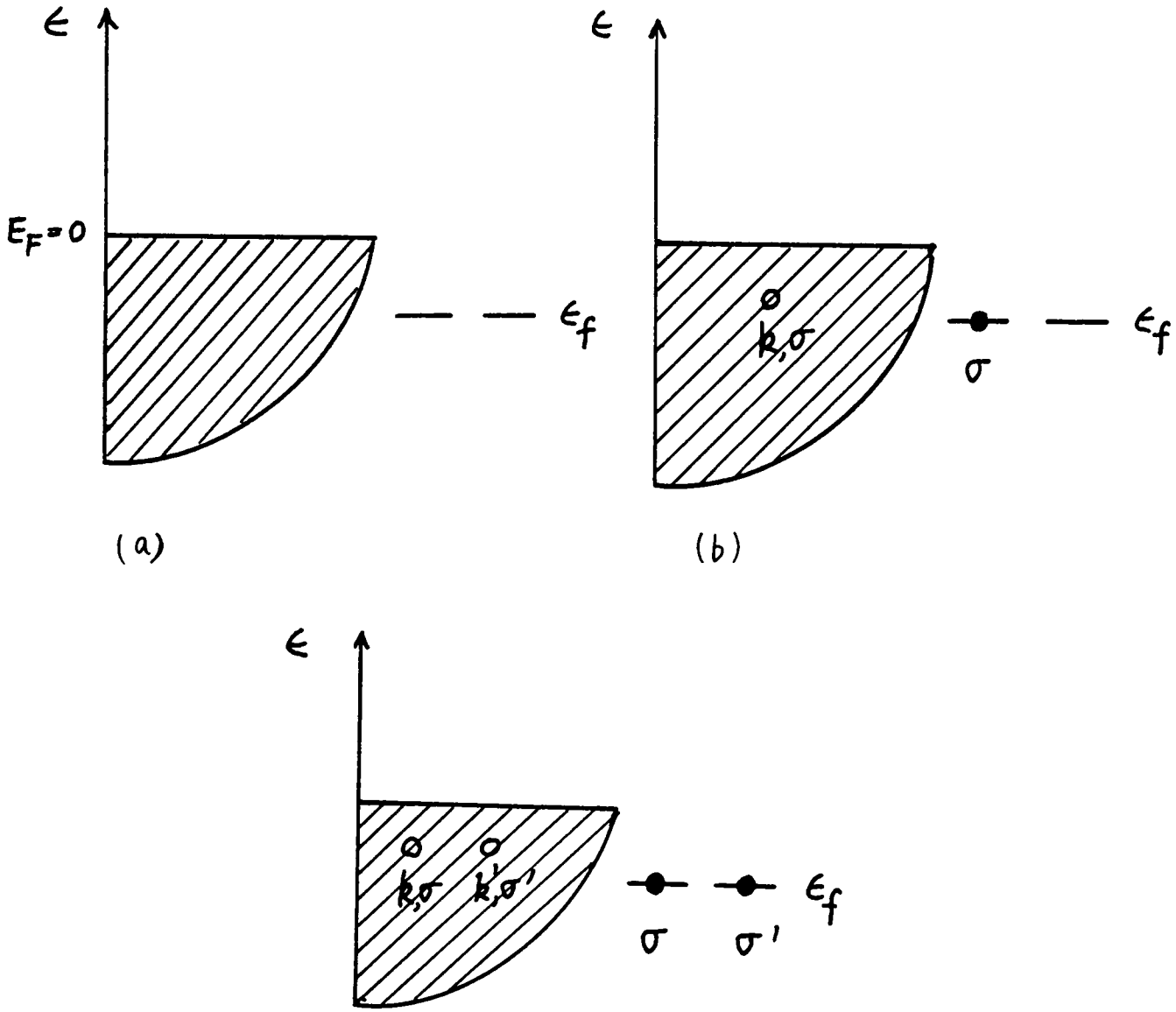
ϵ
$E_F = 0$
ϵ_f
(a)
ϵ
k,σ
σ
ϵ_f
(b)
ϵ
k,σ
k',σ'
σ
σ'
ϵ_f
(c)

Fig. 2

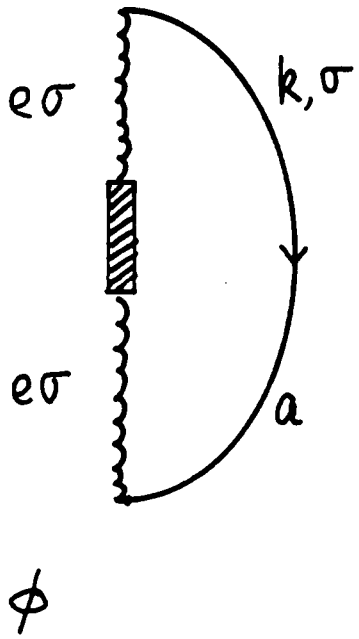

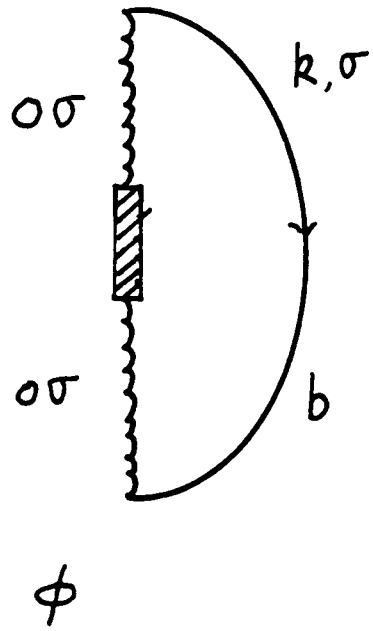

Fig. 3(a)

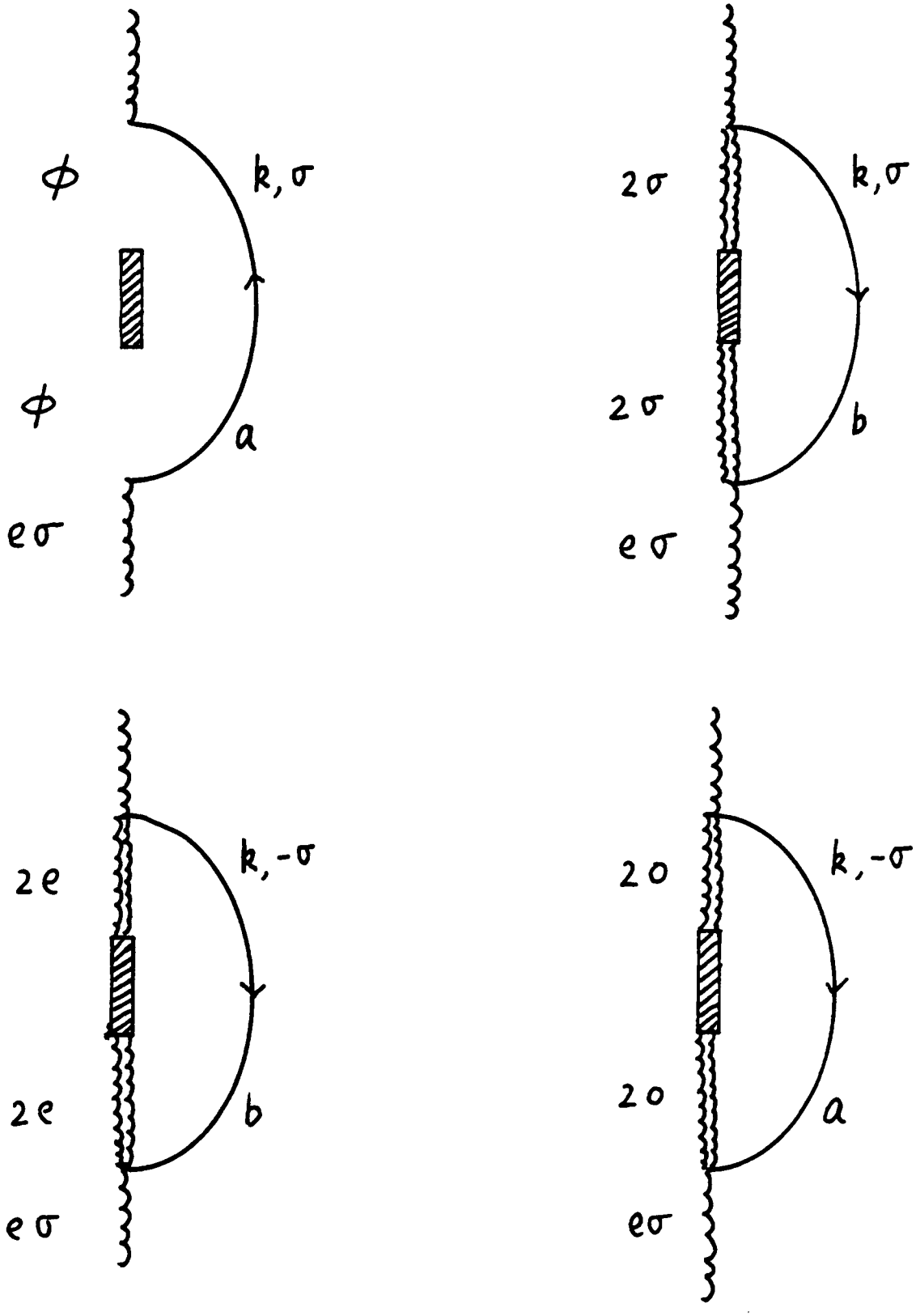

Fig. 3 (b)

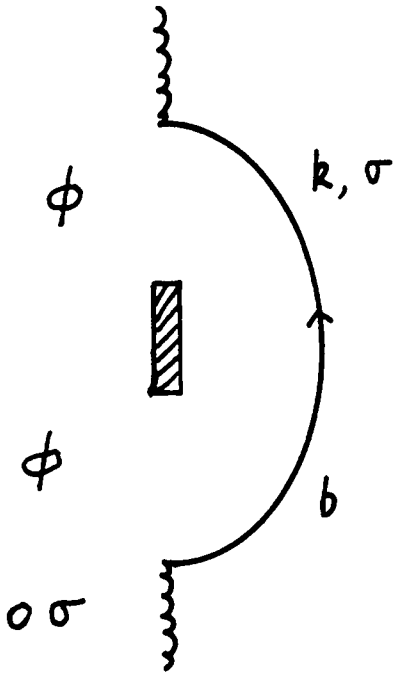

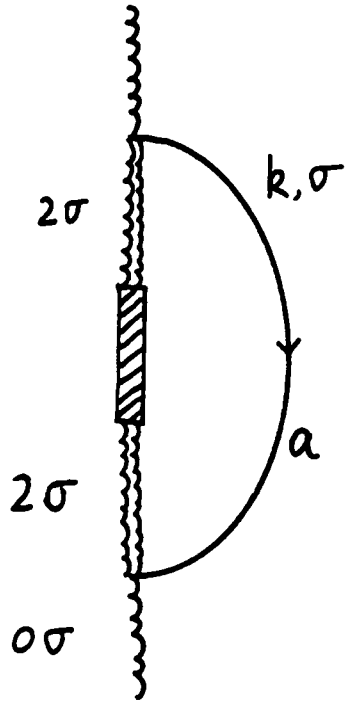

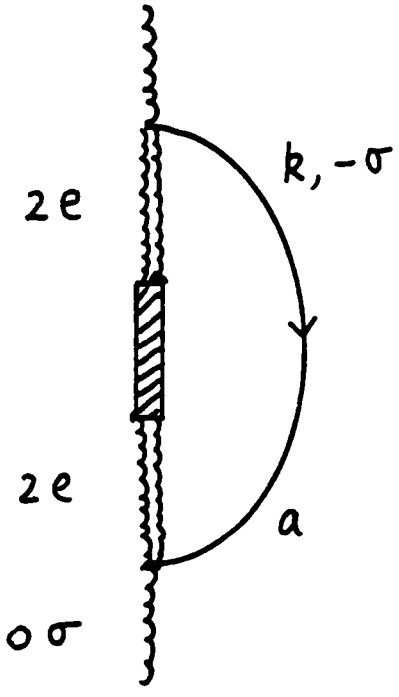

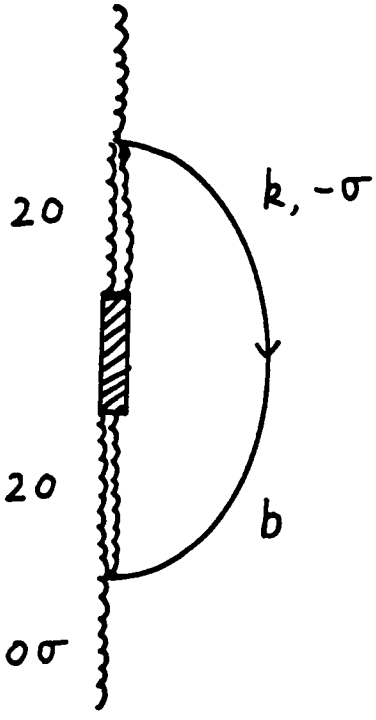

Fig. 3(c)

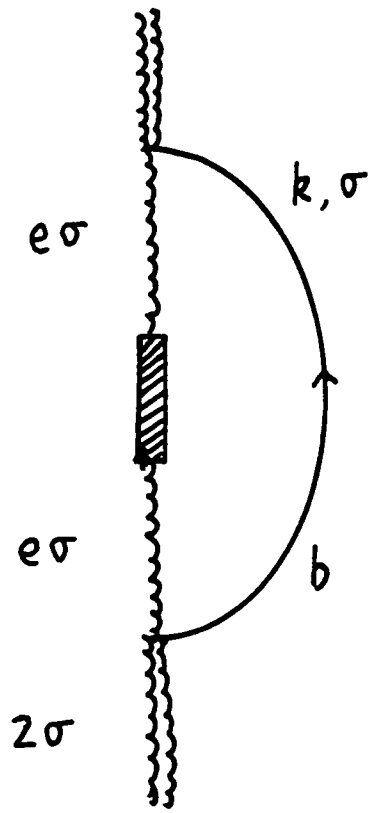

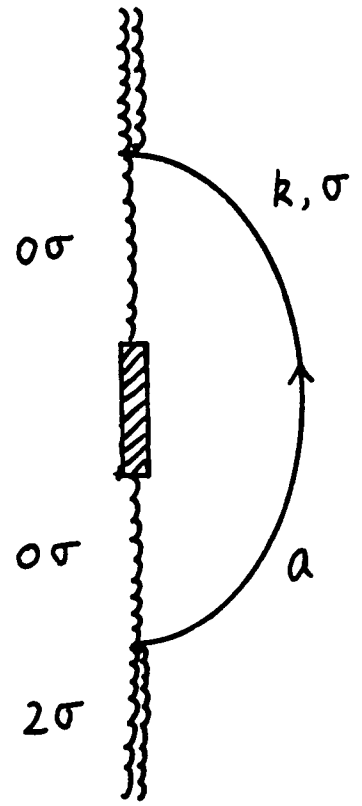

Fig. 3 (d)

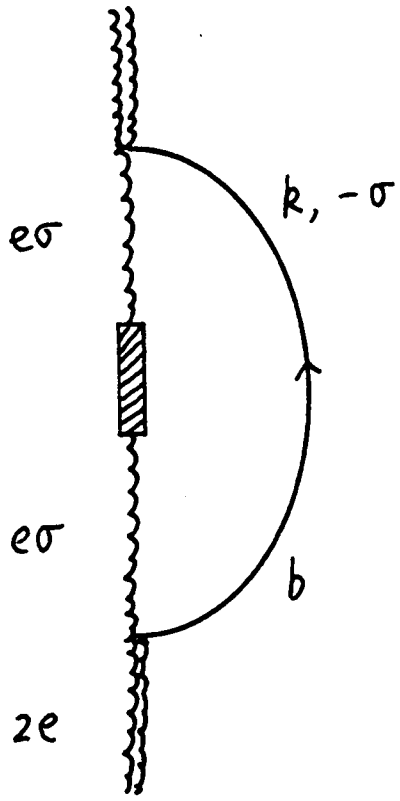

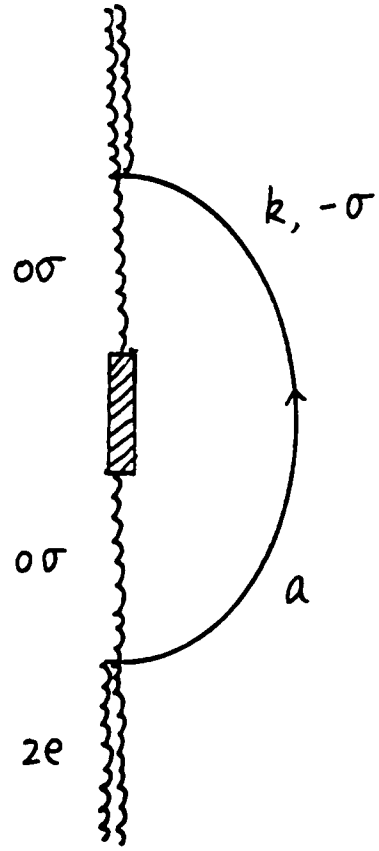

Fig. 3(e)

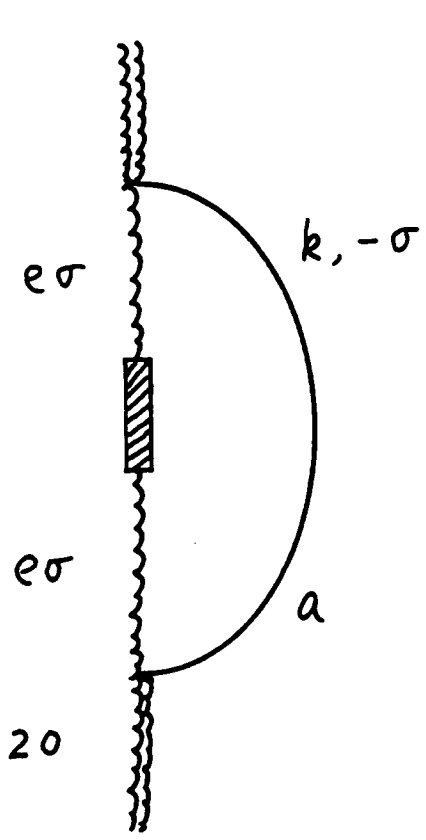

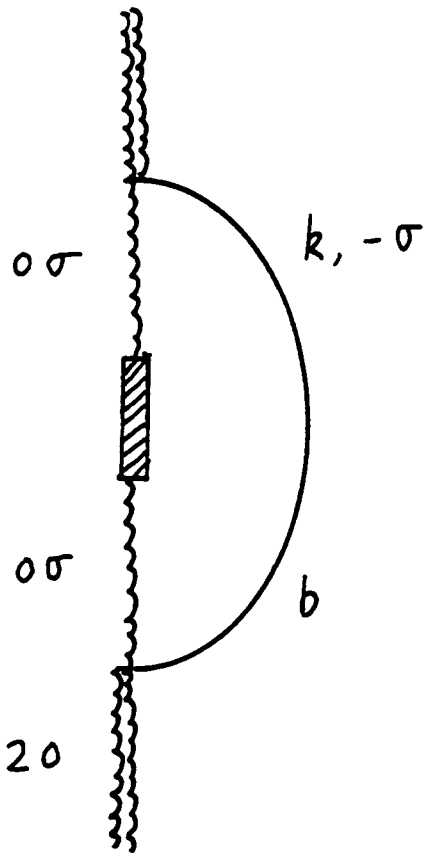

Fig. 3(f)

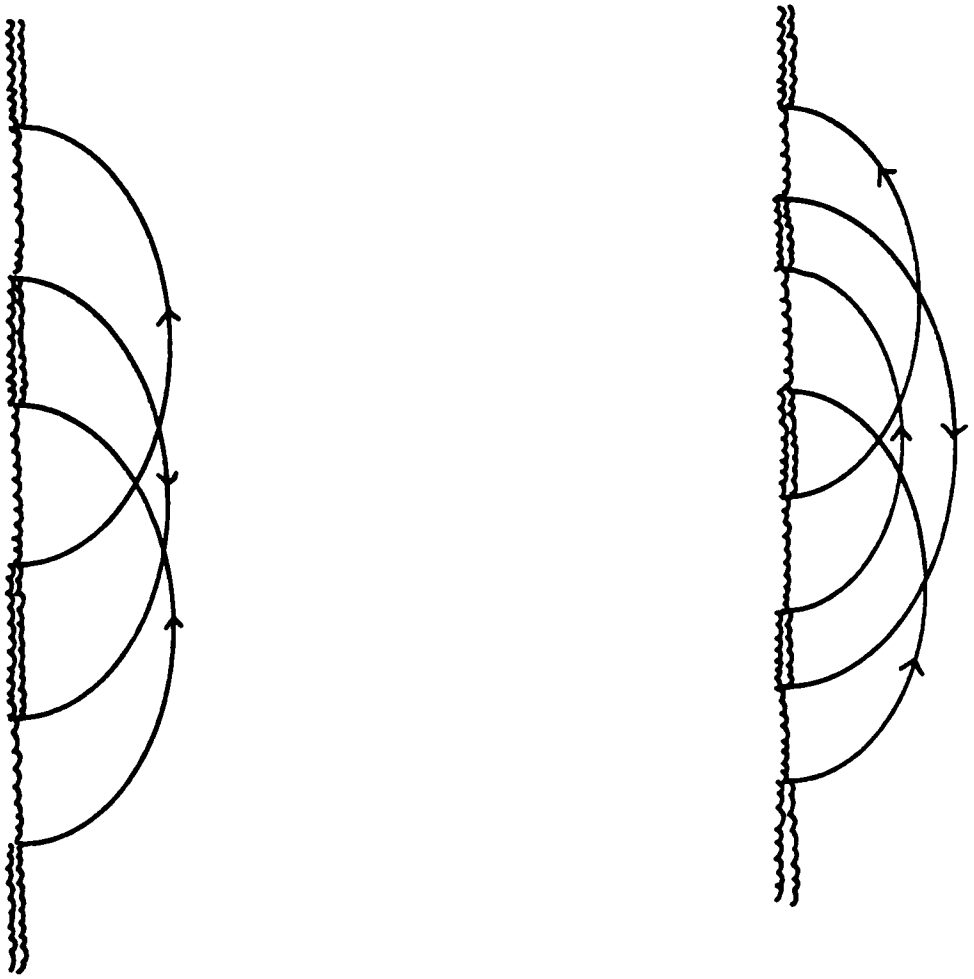

Fig. 4

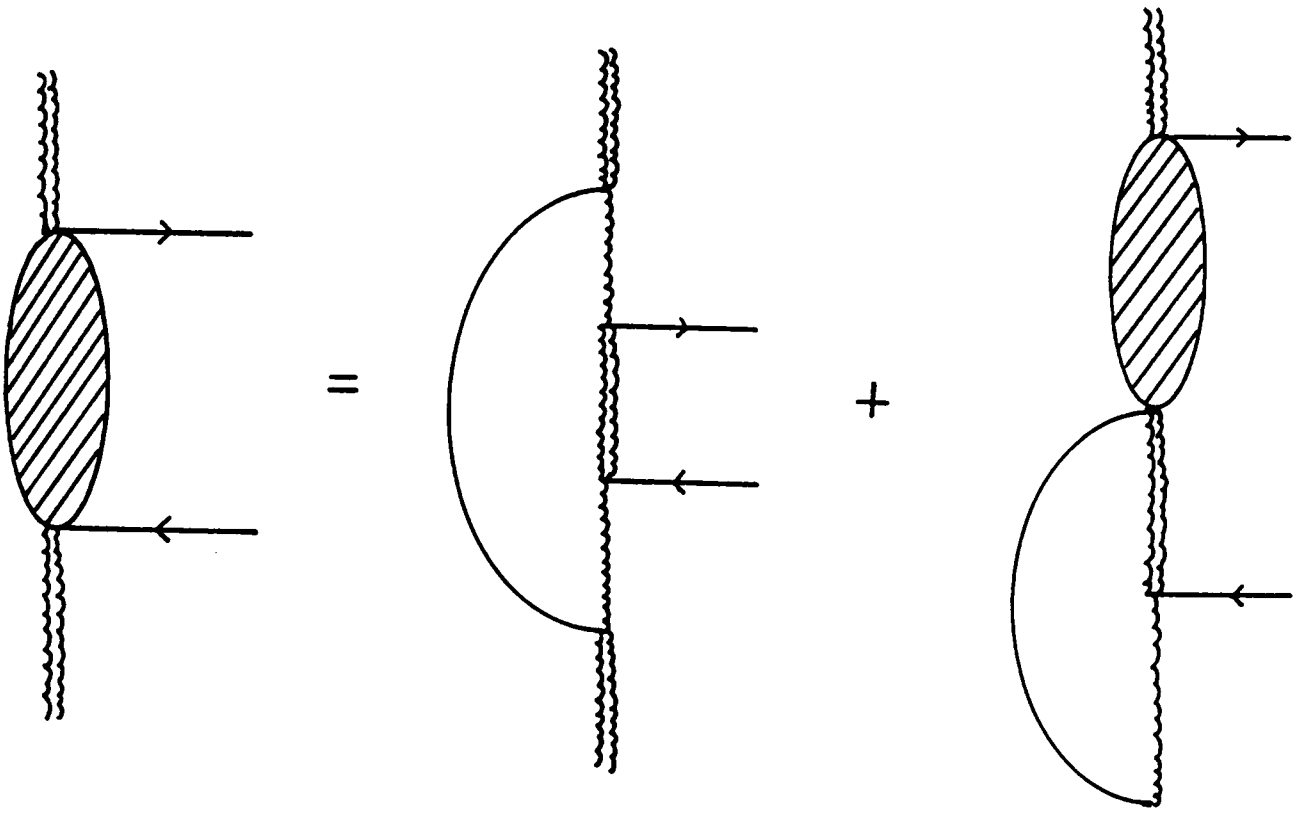

Fig. 5

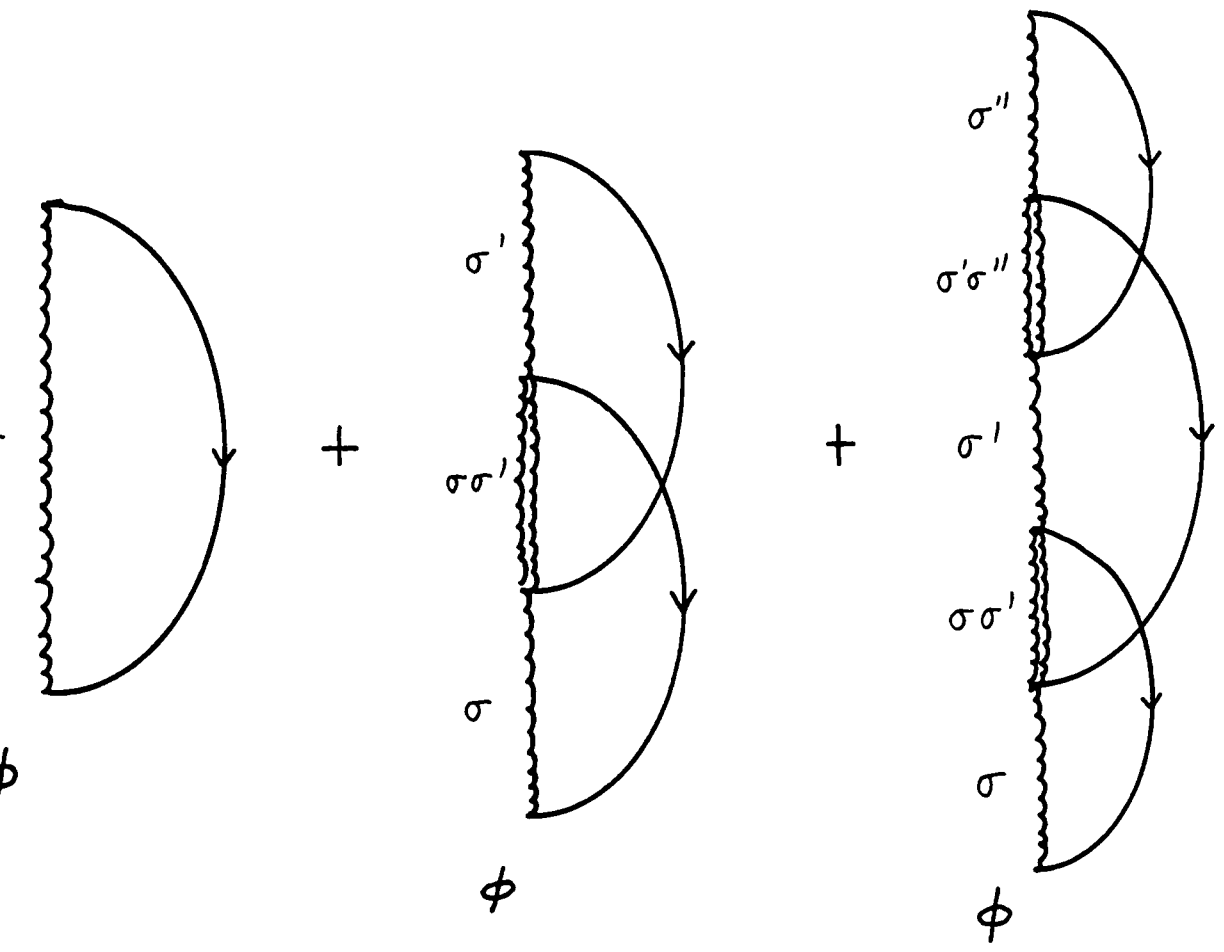

Fig. 6

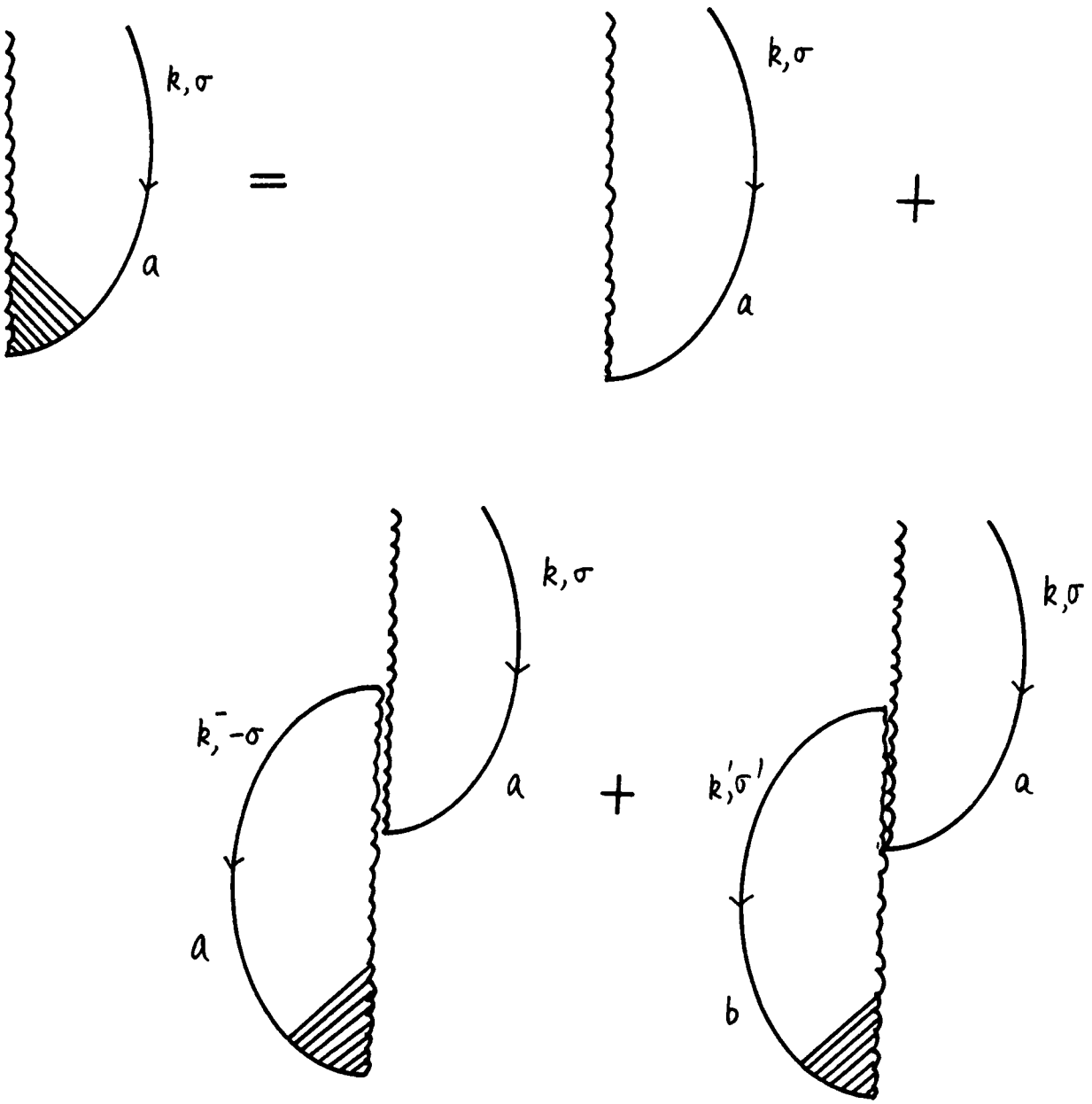

Fig. 7(a)

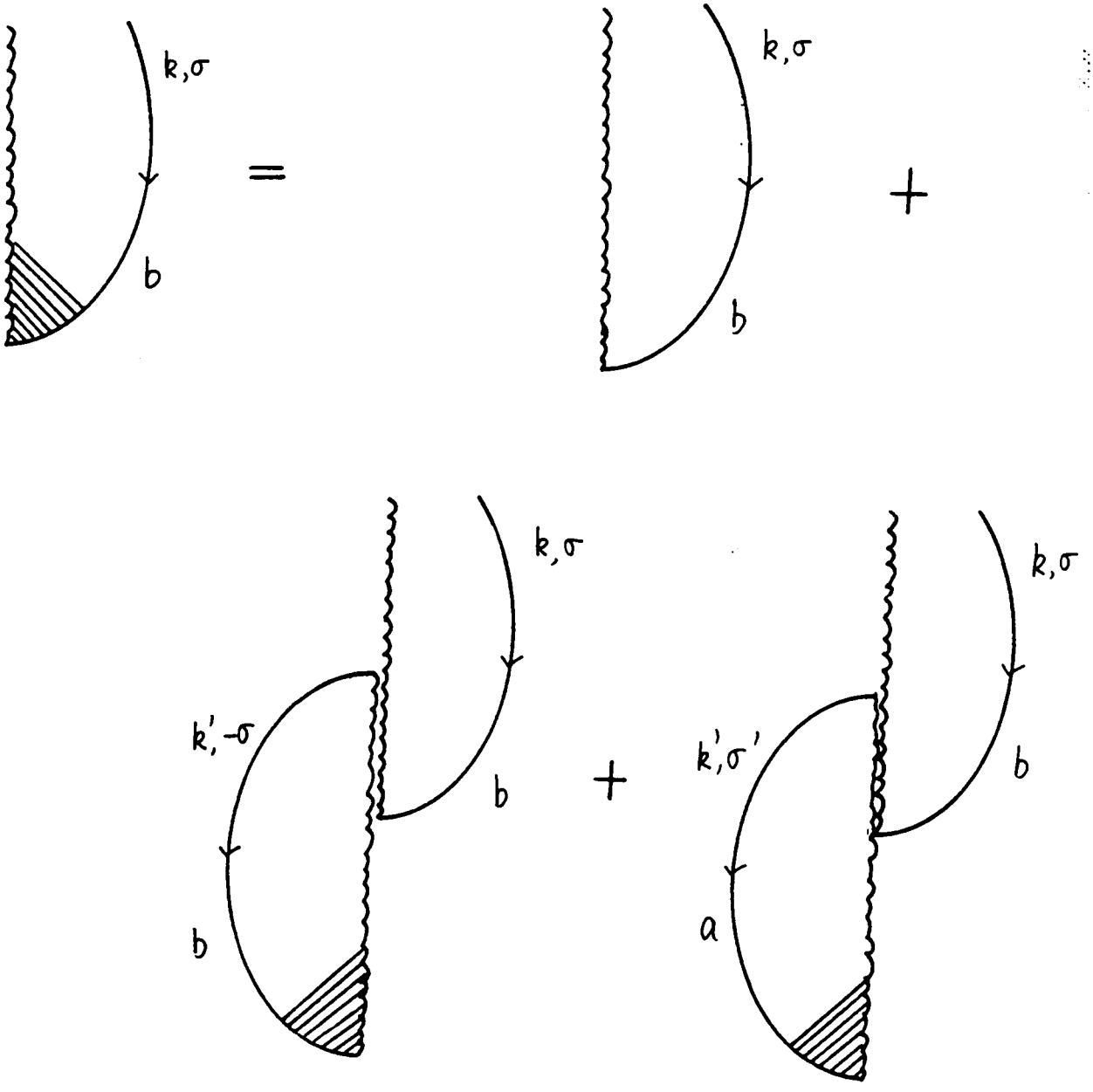

Fig. 7(b)

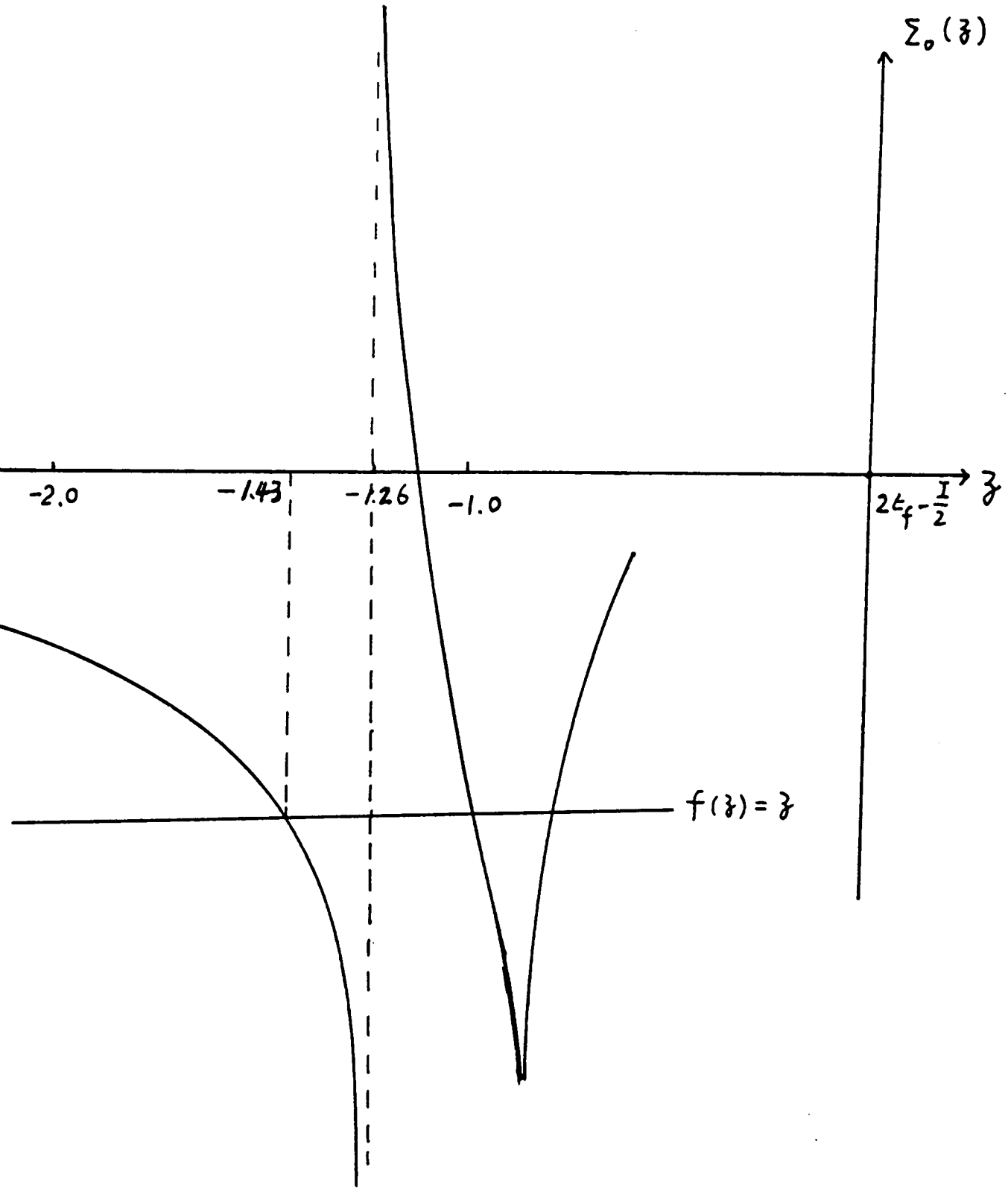

Fig. 8.

I	T_K/I	T_{K+}	T_{K-}	E_0	E_0/T_{K-}
0.1	0.34	0.0065	0.016	-0.031	-1.91
0.2	0.17	0.0023	0.010	-0.017	-1.66
0.3	0.11	0.0015	0.0077	-0.011	-1.43
0.4	0.084	0.00081	0.0064	-0.0084	-1.31

$PV^2 = 1.0$ $\quad \epsilon_f = -6.5$ $\quad D = 22.22$

$\frac{\sin k_F R}{k_F R} = 0.2$ $\quad T_K = 0.0334$

Table 1.

The vita has been removed from the scanned document